

**DEPARTMENT OF PHYSICS
UNIVERSITY OF PUNE**

**M.Sc FINAL SEMESTER PROJECT
on**

**RADIO HOLOGRAPHY
OF
GMRT DISHES**

by

**ABHIRUP DATTA
(Roll - 2002P014)**

**Under the guidance of
PROF. RAJARAM NITYANANDA,
CENTER DIRECTOR,
NATIONAL CENTER FOR RADIO
ASTROPHYSICS
TATA INSTITUTE FOR FUNDAMENTAL
RESEARCH**

Department of Physics

University of Pune

Pune-411007

PROJECT CERTIFICATE: PHY-

1. **Name of the student :** Abhirup Datta
2. **Permanent Address :** 78/G, Brahma Samaj Road,
Kolkata - 700034,
West Bengal.
3. **Permanent Registration No. :** 2002P014
4. **Name of Teacher / Guide :** Prof. Rajaram Nityananda
Center Director, NCRA-TIFR
5. **Period of Project Work :** 6 Months
6. **Title of the Project :** Radio-Holography of GMRT Dishes.
7. The project was carried out by the candidate ALONE
8. I declare that the write up is as per suggestions at the backsides and the Chapters 3 onwards refer mainly to the work I have carried out as my project.
In my view, it has roughly the following structural weightages in %.(Total - 100%)

Weightages

I) Theoretical

- | | |
|--|------|
| (a) Literature review | 20 % |
| (b) Theoretical calculations based on
available literature. | 20 % |
| (c) New theory and calculations | % |

II) Experimental

- | | |
|---|------|
| (a) Equipment development | 30% |
| (b) Repeat work on that available in
literature. | % |
| (c) New work | 30 % |

(Abhirup Datta)
Signature of Student

Remarks of the Teacher

- about % weightage -
- about regularity and capabilities, etc (during the project work) -

Declaration of the Teacher

I have checked that the report is written in the format suggested.
I certify that the student is a regular student of the Department of
Physics and has carried out the project, during that period.

Prof. R. Nityananda
Center Director,
NCRA-TIFR, Pune - 411007.

Prof. D.S. Joag
Head, Department of Physics
University of Pune, Pune-411007.

M.Sc Project Report must be in the following form:-

1. Title exactly indicating and emphasizing the student's work and special contributions of the student.

2. About two to five page chapter wise summary is essential. More emphasis to be given on new facts that the student has studied, over the above regular study he has carried out in other courses. (References to page or article numbers in your text where the details can be found are essential in this summary).

3. Detailed content which give the information, complementary to summary. This may have the following sequence :-

(a) Acknowledgements .

(b) Introduction to the subject, mainly sort of background literature survey.

(c) Exact aim of the student's study.

(d) Student's own study and experimentation.

(e) Discussion, concluding remarks of the same.

(f) Reference list (as in research papers) *(All these references must have been referred in your text)

4. Note that the project report must be written with the examiner in mind, particularly the short time he may have for examining the same; e.g. the figures and tables must have good indicative captions. Similarly even in case, the project is carried out jointly, the reports must be written independently giving one's own contribution and views.

*

(1) For book : "Author's Name ", "Title of book ", Vol No. Edition (Mention Cheap Edition/Student Edition), Publisher's name, Year of Publication, Chapter No, Page nos.

(2) For Research paper or article in journal or magazine :
"Author's name , "Title of the paper " , name of the journal (country),
Vol.No. pp, Months, Year.

RADIO HOLOGRAPHY OF GMRT DISHES

Abhirup Datta^{*1}

¹ Department of Physics, University of Pune, Pune 411007, India

Contents

1	Chapter1: Need for Radio-Holography GMRT Dishes	1
1.1	Overview of GMRT	1
1.2	Design of GMRT Dishes	1
1.3	Nomenclature of the 30 Antennas	3
1.4	Surface Error Measurement	3
1.5	Need for Radio-Holography	4
2	Chapter2: Radio-Holography - An Introduction	5
2.1	Definition in Optical Wavelength	5
2.2	Definition- in Radio Wavelength	5
2.3	Different kinds of Radio-Holography	5
2.3.1	Full-Phase Holography	6
2.3.2	Shearing Holography	6
2.3.3	Phase-Retrieval Holography	7
2.3.4	Laser Metrology	7
3	Chapter3: Theory of Radio-Holography	9
3.1	Aperture-Distribution vs Far Field Pattern	9
3.2	Fraunhofer Diffraction at Aperture	9
4	Chapter4: Data Acquisition Technique	11
4.1	Frequency of Observation	11
4.2	Choice of the Source	11
4.3	Scheme	11
4.4	Nyquist Sampling Theorem	13
4.5	Determination of Scan Rates	14
5	Chapter5: Data Analysis	15
5.1	Self-Consistency Check	15
5.2	Channel-Collapse and Band-Pass Calibration	15
5.3	Smoothing the Data	17
5.4	Transforming from Far Field to Aperture Field	19
6	Chapter6: Results and Measurement of Surface Errors	21
6.1	Measurement of Surface Errors - Theory	21
6.2	Image of Dish	22

6.3	Self-Consistency Checks	35
6.3.1	Theory	35
6.3.2	Results for C03	35
7	Chapter7: Measurement of Defocus	36
7.1	Theory for measuring the defocus	36
7.2	Analysis	38
7.3	Results for C03	38
8	Chapter8: Holography at 610 MHz	39
8.1	Scanning Technique	39
8.2	Results	40
9	Chapter9: Second Observation at 1280 MHz	43
9.1	Scanning Technique	43
9.2	Results	44
9.3	Estimate of Coma	44
10	Chapter10: Further Development	49
11	Chapter11: Codes	50
11.1	Fortran Code for Scanning Technique	50
11.2	Octave Code for Data Analysis	54
11.2.1	Initial Analysis	54

Acknowledgement

The present report is regarding the Radio-Holography of the GMRT Dishes under the guidance of Prof. Rajaram Nityananda, Center Director, NCRA, India. This project is a part of my M.Sc Physics course at Department of Physics, University of Pune and is mandatory for the partial fulfillment of my M.Sc degree.

Working with Prof. Rajaram is a wonderful experience and an excellent opportunity to me for which I am really grateful to him. I should also mention my extreme gratitude to Prof. S. Ananthakrishnan , Observatory Director, GMRT. It is due to him I got a chance to work at NCRA. And my project with Prof. Rajaram is an outcome of his suggestion.

I am also grateful to Prof. A.P.Rao for his valuable suggestions regarding the development of this project. Besides, I am also thankful to all the students, faculties and staff members of NCRA and GMRT for helping me in my project in different aspects.

Chapter 1

Need for Radio-Holography GMRT Dishes

1.1 Overview of GMRT

The Giant MeterWave Radio Telescope(GMRT) is one of the largest Radio Telescopes in the world. GMRT is a unique facility for radio astronomical research using the metrewavelengths range of the radio spectrum,operating in the frequency range of about 50 to 1500 MHz . It is located at a site about 80 km north of Pune. GMRT consists of 30 fully steerable gigantic parabolic dishes of 45m diameter each spread over distances of upto 25 km.The number and configuration of the dishes was optimized to meet the principal astrophysical objectives which require sensitivity at high angular resolution as well as ability to image radio emission from diffuse extended regions. Fourteen of the thirty dishes are located more or less randomly in a compact central array in a region of about 1 sq km. The remaining sixteen dishes are spread out along the 3 arms of an approximately ‘Y’-shaped configuration over a much larger region, with the longest interferometric baseline of about 25 km.

1.2 Design of GMRT Dishes

The construction of 30 large dishes at a relatively small cost has been possible due to an important technological breakthrough achieved by Indian Scientists and Engineers in the design of light-weight, low-cost dishes. The design is based on what is being called the ‘SMART’ concept - for Stretch Mesh Attached to Rope Trusses. The dish has been made light-weight and of low solidity by replacing the conventional back-up structure by a series of rope trusses (made of thin stainless steel wire ropes) stretched between 16 parabolic frames made of tubular steel. The wire ropes are tensioned suitably to make a mosaic of plane facets approximating a parabolic surface. A light-weight thin wire mesh (made of 0.55 mm diameter stainless steel wire) with a grid size varying from 10 X 10 mm in the central part of the dish to 20 X 20 mm in the outer parts, stretched over the rope truss facets forms the reflecting surface of the dish. The low-solidity design cuts down the wind forces by a large factor and is

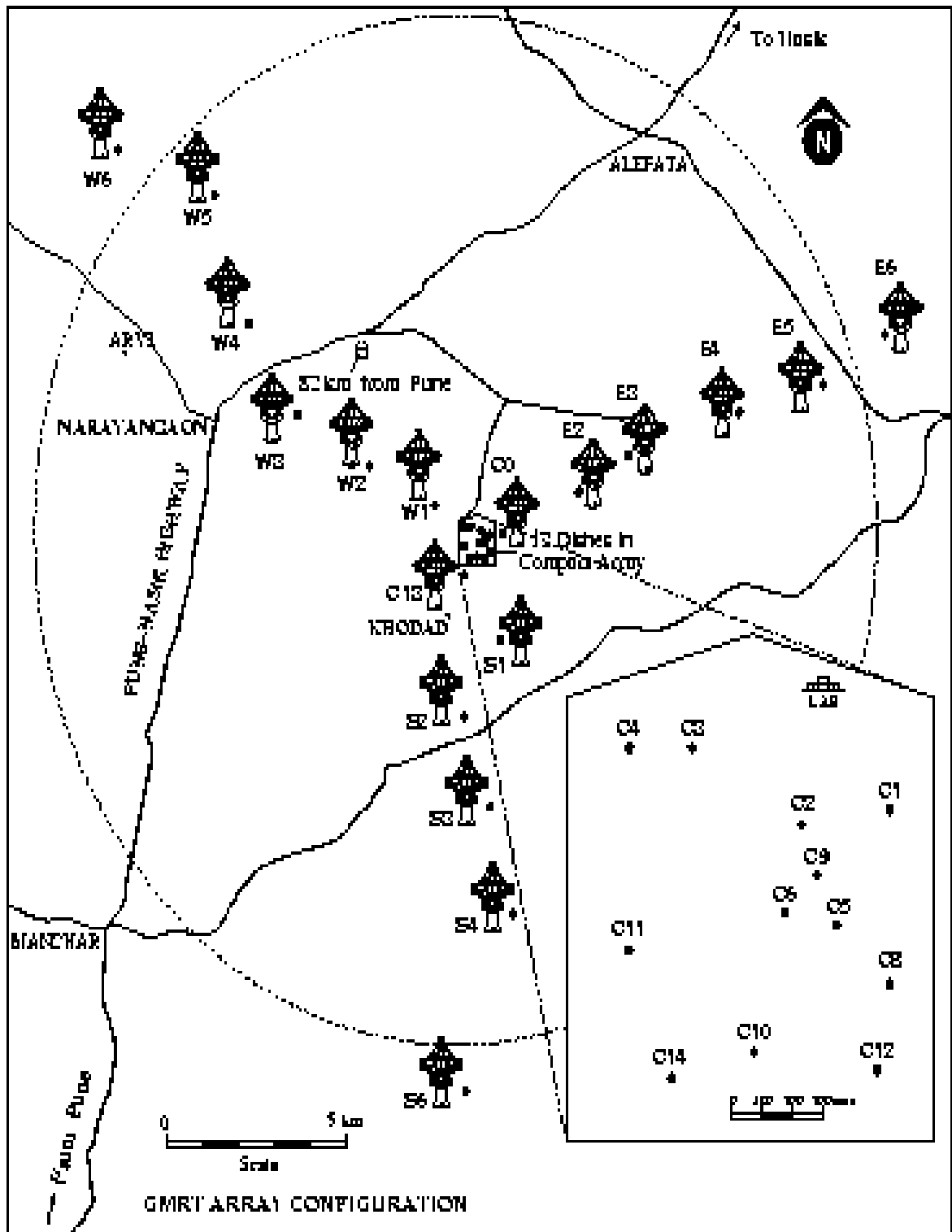


Figure 1.1: Configuration of GMRT Antennas in the 'Y' shape

particularly suited to Indian conditions where there is no snowfall in the plains. The overall windforces and the resulting torques for a 45-m GMRT dish are similar to those for only a 22-m dish of conventional design, thus resulting in substantial savings in cost. The dish is connected to a 'cradle' which is supported by two elevation bearings on a yoke placed on a 3.6 m diameter slewing-ring bearing secured on the top of a 15 metre high concrete tower. The weight of the disk is about 80 tonnes and the counter-weight is about 40 tonnes. The dishes have alt-azimuth mount.

1.3 Nomenclature of the Antennas

The antennas at GMRT has been named in order to facilitate the observation and data analysis procedure. The 'Y' shaped array has been formed with 14 antennas near the central region (named Central Square) and the remaining 16 are divided into 3 arms which form almost a 'Y' shaped figure.

The central square antennas are named from C00 to C14 (with the exception of C07). So in total there are 14 antennas in the central square. The 3 arms are named East(E), West(W) and South(S). They have antennas named as E02, E03, E04, E05, E06, S01, S02, S03, S04, S06, W01, W02, W03, W04, W05 and W06.

1.4 Surface Error Measurement

During the construction of each of these gigantic 45m dishes, the whole of it was not built at the top of the 15m tower. Instead the inner portion was only built at the top, while the outer part was built at the ground and later fitted with the inner portion on the top. So the original paraboloid design of the surface might have got hampered due to these mechanical fitting reasons. So there is a need to measure the surface errors of the GMRT dishes in order to estimate the deviation from the ideal parabolic surface.

There are also other ways in which the surface may get distorted from its parabolic nature. It may happen due to gravitational effects, wind force, unequal heating of the sun, etc.

After the construction of each dish theodolite measurement has been conducted over almost all dishes. But the measurement with theodolite is a very time consuming process. It took almost 3 - 4 days to measure a single dish. Moreover the measurements were taken only pointing the antennas towards the zenith. So the effect of gravity on the deformation cannot be taken into account. But the major drawback of the theodolite measurement has been that it is difficult to make repeated measurements.

1.5 Need for Radio-Holography

Radio-Holography is very powerful technique to measure the surface errors of the dishes. This process not only can predict about the surface errors but also predict about the errors in the feed-positioning, etc. It is a much faster method as compared to theodolite measurement. The estimated time required to complete the measurement on all 30 dishes is 2 days(approx.) as compared to about 2-3 months in case of theodolite measurement. Moreover Radio-Holographic technique involves more on software than on mechanical aspects so holography does not require the amount of man power required by the theodolite measurement. And the cost of doing a Holographic measurement is much less as compared to that of a Theodolite measurement.

Chapter 2

Radio-Holography - An Introduction

2.1 Definition of Holography in Optical Wavelengths

The optical recording of the object wave formed by the resulting interference pattern of two mutually coherent component light beams. In the holographic process, a coherent beam first is split into two component beams, one of which irradiates the object, the second of which irradiates a recording medium. The diffraction or scattering of the first wave by the object forms the object wave that proceeds to and interferes with the second coherent beam, or reference wave at the medium. The resulting pattern is the three-dimensional record (hologram) of the object wave.

2.2 Definition- in Radio Wavelength

In radio astronomy, a method for refining the feed and panel alignment, thus for improving the aperture efficiency or antenna gain of a radio telescope. By scanning an antenna's beam over a raster around an unresolved radio source, and using another antenna pointing at the same source as a reference, information is obtained about the amplitude and phase distributions of the signal reflected from the antenna surface. These distributions are used to specify corrections (if needed) for the focus and alignment of the feeds or of the positions of individual panels in the reflector.

2.3 Different kinds of Radio-Holography

In order to achieve an aperture efficiency of 50 %, a radio telescope must have a surface accuracy of $\lambda/16$, where λ is the observing wavelength. In this section we mention few kinds of Surface error measurement techniques[11]. Among them, except Laser Metrology all other techniques are based upon the principle that one can derive the shape of an antenna's primary from the amplitude and phase of its beam pattern on the sky [8]. The complete shape requires measuring the beam pattern over the full half-sphere. If the measurement is restricted to N beamwidths i.e. an angle of $N\lambda/D$ where D is the diameter of the primary, the shape is determined with a spatial resolution of $\sim D/N$. The

beam pattern need not be measured with a monochromatic source so long as the spectral resolution ($\lambda/\Delta\lambda$) is not so small as to smear the measurements over the aperture by more than the spatial resolution. Thus the spectral resolution should be larger than N .

2.3.1 Full-Phase Holography

Full-Phase Holography is the most mature of the techniques discussed here[9].

This technique requires a transmitter to illuminate the antenna to be measured. The antenna is scanned across the transmitter to measure the beam pattern of the antenna. A reference antenna which also receives the transmitter signal is needed in order to provide a phase and amplitude reference. The output of the two receivers when combined gives both the amplitude and phase of the beam pattern of the antenna to be measured. This can be used to derive the amplitude and relative phase of the radiation reflected from points on the antenna surface when the antenna is pointed directly at the transmitter. An antenna with a perfect figure in perfect focus would have all these reflections in phase with each other. The amount that the reflections are not in phase measures the deviations of the surface from a perfect figure.

Atmospheric scintillation effects can induce an artificial phase difference between the reference antenna and the antenna to be measured. This effect on the measurement will be minimized if the separation between the 2 antennas is minimized. The measurement of the telescope is best done in the configuration that is normally used for observations.

While all the holography techniques give very accurate results, they do not allow one to measure the focal length of the telescope directly. Instead they tell one how to optimize the positions of the panels for whatever mean focal length the panels happen to define. If the focal length is not what was intended when the panels were fabricated, one will be led to bend the panels so as to achieve the erroneous focal length.

2.3.2 Shearing Holography

Shearing holography is an alternate method of measuring an antenna's surface. Instead of measuring the amplitude and phase of the beam pattern on the sky, it measures these in the focal plane (which is equivalent to measuring the beam pattern). This focal pattern of a transmitter or celestial object can also be Fourier Transformed to yield the surface errors of the telescope primary [12]. Instead of measuring the pattern's amplitude and phase directly, an interferometer with a beam splitter is used to superimpose the on-axis (reference) pattern with an off-axis pattern. The resulting interference pattern is focused on a single-pixel detector. A grid of such measurements at different off-axis points can be used to derive the surface error map of the telescope.

An advantage of this technique over full-phase holography is that it does not require a reference receiver. And since only a modest frequency resolution ($\lambda/\Delta\lambda$) of about 20 is needed and only the power need be measured, the detector can be a bolometer. One can either use a narrow band filter to achieve this resolution or, by adding the capability of moving one of the flat mirrors in the interferometer to change the relative path length of the two arms of the interferometer, the interferometer can be used as a Fourier transform spectrometer. This mirror was scanned at each point in the measurement to synthesize a spectrum.

2.3.3 Phase-Retrieval Holography

Phase retrieval holography (also known as out-of-focus holography) is another alternate method of measuring the surface errors of a radio telescope [10]. An advantage of this technique is that it is done by simply comparing observations of a point source both in focus and after moving the telescope out of focus by a known amount. (In practice, one obtains more reliable results if one has observations at several different focus positions.) Like with Shearing Holography, the point source need not be monochromatic. That is, no special holography receiver or modifications to the telescope are required. Since there are no phase measurements made, the phase must be in effect retrieved in the analysis of the data. One disadvantage is that since no phase is measured directly, the problem is non-linear and one cannot solve directly for the surface error map. Instead, one must propose a model of the surface errors and find the best set of model parameters that will fit the data.

With both Shearing Holography and Phase-retrieval Holography, one need not use a transmitter but instead use can an astronomical continuum source (so long as it is not too extended). This has the advantage that the shape of the telescope primary need not be measured with the telescope pointing near the horizon as is the case with a measurement technique with a transmitter on the ground. A disadvantage is that one is limited by the signal to noise ratio one can achieve on the astronomical object. Even the brightest continuum sources cannot achieve the signal to noise one can obtain with a holography transmitter. So the size of the resolution element on the telescope aperture of the resulting surface error map, is larger than that normally achieved with a transmitter.

2.3.4 Laser Metrology

Another method of measuring the surface of an antenna is laser metrology. Laser rangefinders are used to measure the distance of retroreflectors mounted on the surface. A minimum of three laser rangefinders is needed to define the position of a retroreflector in three dimensions but more accurate results are obtained if there are more than three laser rangefinders. An advantage of this technique is that it can be done while the telescope is being used for normal observing.

A disadvantage is that retroreflectors must be permanently mounted on the surface and their positions measured relative to the panels.

The GBT(GreenBank Telescope) and the LMT(Large Millimeter Telescope) plan to use this method to measure and correct the errors in their primaries in real time. Tests of the method for the GBT are promising, but an actual measurement of its surface via laser rangers has not yet been one. The measurement errors are expected to be under $100 \mu m$ but will probably be considerably larger than obtained via holography techniques.

Chapter 3

Theory of Radio-Holography

Radio-Holography exploits the Fourier-Transform relationship between the Aperture-field Distribution and the Far-field pattern(or the focal plane distribution)

3.1 Aperture-Distribution vs Far Field Pattern

Let the Far-field Pattern be given by :-

$$V(\theta, \phi) = v(\theta, \phi) \exp[\Phi(\theta, \phi)] \quad (3.1)$$

Let the Aperture-field Pattern be given by :-

$$A(x, y) = a(x, y) \exp[\Phi(x, y)] \quad (3.2)$$

Then the relation between them is given by the Fourier-Transform:

$$A(x, y) = \int \int_{-\infty}^{\infty} V(\theta, \phi) e^{-j2\pi(\theta x + \phi y)} d\theta d\phi \quad (3.3)$$

where $x, y \Rightarrow$ coordinates on the dish

$\theta, \phi \Rightarrow$ coordinates on the sky-plane.

This $V(\theta, \phi)$ is necessarily a complex voltage \rightarrow which has to be measured in the interferometric mode.

It is noteworthy here, that equation 3.3 is similar to the expression we encounter for Fraunhofer Diffraction at the aperture.

3.2 Fraunhofer Diffraction at Aperture

In context to the Fraunhofer diffraction field let us have an aperture illuminated by an electromagnetic field of amplitude $E(l, m)$ where l, m are direction cosines. If (x, y) plane is in the far field of this aperture then the wavefront is plane in the (x, y) plane.

Let P_1 be a point in the (x,y) plane. Then the radiated field from the aperture will have a distribution at P_1 , when integrated over the entire aperture, as [1]:

$$\tilde{E}(x, y) = \frac{e^{-j2\pi\nu(t-\frac{R}{c})}}{R} \int \int_{\text{aperture}} E(l, m, t - \frac{R}{c}) e^{-j2\pi(\frac{x}{\lambda}l + \frac{y}{\lambda}m)} dldm \quad (3.4)$$

Now, time dependant fields are replaced by their r.m.s field amplitudes.

$$\tilde{E}(x, y) \propto \int \int_{\text{aperture}} E(l, m) e^{-j2\pi(\frac{x}{\lambda}l + \frac{y}{\lambda}m)} dldm \quad (3.5)$$

Chapter 4

Data Acquisition Technique

This chapter deals with the technique that was followed while taking the holographic-observation using GMRT. The basic strategy that is adopted here is influenced by the technique developed by Scott and Ryle(1957).

4.1 Frequency of Observation

The frequency of observation was chosen to be 1280 MHz(L- band) ($\lambda = 24.3$ cm). In this band the primary beam was reported to be 0.4° i.e. 24 arcmin. Whereas at other bands it is much higher. So in order to reduce the time of observation we have chosen L-Band.

4.2 Choice of the Source

The source to be observed is chosen to be 3C147. It is one of the brightest source and one of the flux calibrators that radio-astronomers often use. It is also a point object so it meet our needs of a source that will not be resolved out at longer baselines. The flux of 3C147 is about 22.5 Jyat 20 cm. Whereas the nearest bright source at 20cm is 3C286 which has a flux density of $15Jy$ at 20 cm.

4.3 Scheme

We have chosen 2 antennas as reference ones (C00 and C10),. These reference antennas will only track the source throughout the observation. While the remaining 28 antennas will be tracking a circular region across the sky in the following fashion:

All of these 28 tracking antennas will scan over a circular region across the sky which has a radius of 3 beamwidths. This extent of 3 beamwidths is chosen at present to reduce the total duration of observation. If the number of beamwidths are increased we will be able to get a better resolution on the dish. Presently with this total 6 beamwidths scans we will be able to get a resolution

of about 7.5 m on the dish (since the resolution is defined as $\frac{D}{n} = 7.5m$). The scheme of the observation is also explained in the Fig: 4.1 .

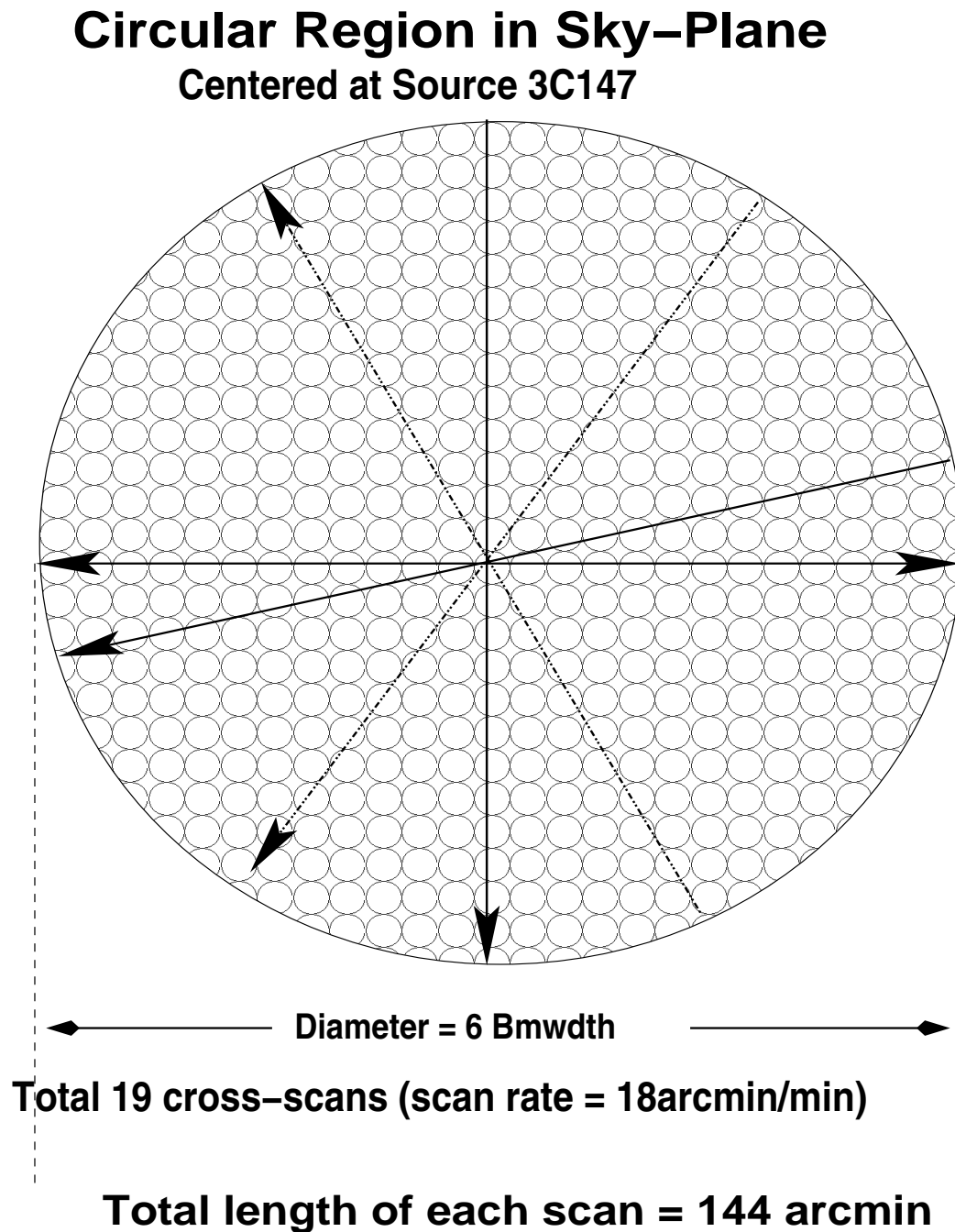


Figure 4.1: Illustration of Scanning Technique

The tracking antennas will start from the periphery of the circular region on sky and then will cross the source which will be at the center of the circular region and will go same distance on the other side of the source. The next scan will

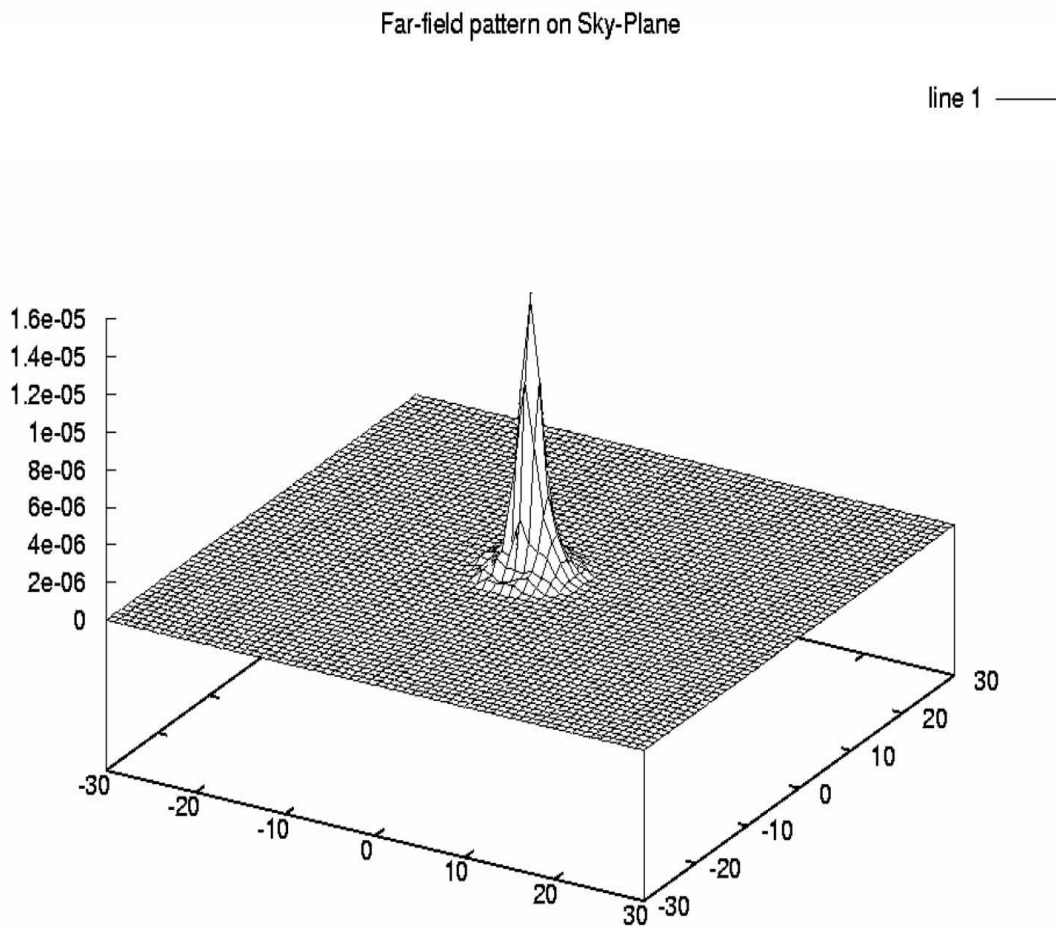


Figure 4.2: Far-Field Pattern - as observed on the sky-plane

start just where the last scan has stopped but with an angular displacement of 10° on the circumference. This next scan will scan the source in the reverse direction to that of the previous one. And this same process follows until the scans covers the full circular region and returns with a scan that is just the reverse scan of the first scan. So in total we have 19 scans. Among these 19 scans, the 1st and the 19th are the same scans taken in the reverse directions. This is done just to do some self-consistency checks while analysing the data.

4.4 Nyquist Sampling Theorem

According to the Nyquist Sampling Theorem [3] :- A bandlimited function, confined to size of D , can be reconstructed completely if sampled at angles spaced by under Nyquist Rate of $\frac{\lambda}{D}$ or less.

So following this theorem we fixed the distance between the successive scans on the circumference to be 10° which less the Nyquist Sampling . Hence we can now reconstruct the completely far-field radiation pattern by this number of scans, without losing any information on it.

4.5 Determination of Scan Rates

The Asimuth-elevation scan-rates for GMRT antenna has been calculated by the following formulae:

$$V_{asimuth} = \frac{sign * V * \cos \theta_n}{\cos \varepsilon} \quad (4.1)$$

$$V_{elevation} = sign * V * \sin \theta_n \quad (4.2)$$

where

sign \Rightarrow alternate scans are opposite in direction w.r.t each other.

$$\theta_{(n+1)} - \theta_n = 10^\circ$$

V \Rightarrow resultant scan-rate = 18 arcmin per minute (chosen)

$\varepsilon \Rightarrow$ angle of elevation , calculated from the following formulae [1]:

$$\sin \delta = \sin \mathcal{L} \sin \varepsilon + \cos \mathcal{L} \cos \varepsilon \cos \mathcal{A} \quad (4.3)$$

$$\cos \delta \cos H = \cos \mathcal{L} \sin \varepsilon - \sin \mathcal{L} \cos \varepsilon \cos \mathcal{A} \quad (4.4)$$

$$\cos \delta \sin H = -\cos \varepsilon \sin \mathcal{A} \quad (4.5)$$

where

H \Rightarrow hour-angle

$\delta \Rightarrow$ declination of the source , L \Rightarrow Latitude of GMRT

$\varepsilon \Rightarrow$ elevation , A \Rightarrow asimuth

Chapter 5

Data Analysis

This chapter deals with the procedure followed while analysing the data of the observation mentioned in the previous chapter. This analysis includes the attempt to build a software for GMRT that will be used in further Holographic measurements. This chapter also attempts to propose a basic formalism that should be followed while doing a Holographic Measurement in the Interferometric mode.

5.1 Self-Consistency Check

While taking the observation 19 total scans of 6 beamwidths were taken. Among these the 1st and 19th scans were exactly the same scan but taken in the reverse direction to each other So in order to validate our method of scanning these two scans were used to check the self-consistency(after reversing the last scan). The last scan was subtracted from the first and the resultant was viewed. It gave us a satisfactory result confirming that each scan actually passed through the source in the way the scans were designed in the previous chapter.

5.2 Channel-Collapse and Band-Pass Calibration

In GMRT we have the data of any observation to be taken across a bandwidth of 32 MHz (with the frequency of observation as the central frequency). And this 32 MHz is divided among 256 channels. This 32 MHz is divided into two bands USB(Upper Side Band) and LSB(Lower Side Band), each having 128 channels each. But we have worked with only one of them. So we have essentially 128 channels of data per timestamp. Now in order to increase the Signal-to Noise ratio(SNR) the data was compressed(averaged) over all the 128 channels.

But while averaging over all the channels we cannot simply take a mean of the data across the channels. Since there is phase variation across the channels so if we take the simple mean then we will lose the information. Hence we follow a technique called BandPass Calibration in order to do so.

BandPass Calibration - Bandpass calibration is necessary to correct for complex gain variations as a function of frequency. The shape of the bandpass is determined by the baseband filters as most other components have a flat response as a function of frequency. Across the bandpass, there is almost a linear phase slope of a few degrees per MHz. The channel-to-channel amplitude variations are of order 0.1-1 percentage. Some antennas show a larger, few percent, amplitude ripple with an approximate width of 3 MHz

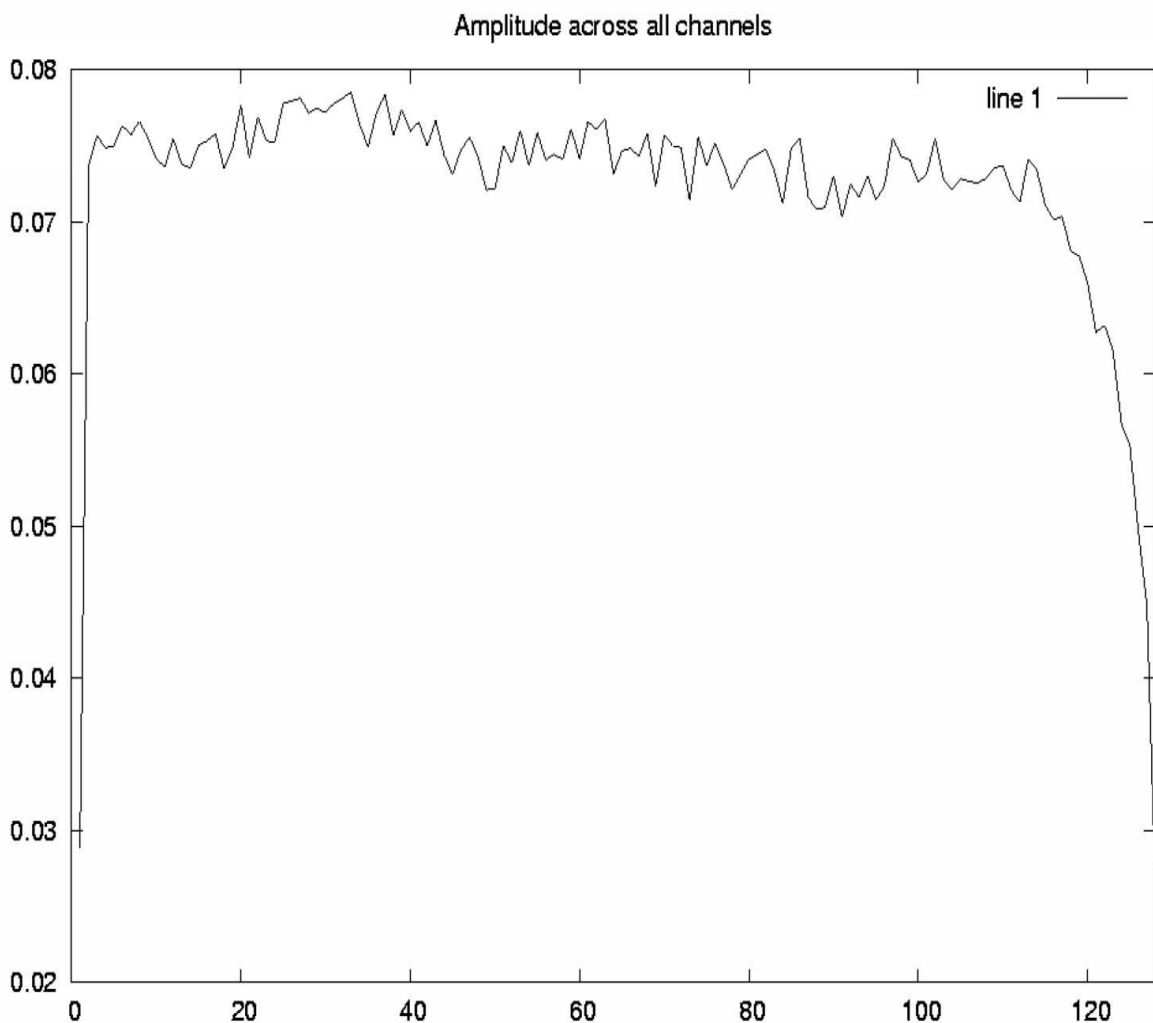


Figure 5.1: Variation of amplitude across all channels at 130

The basic procedure that was followed is as follows :-

- Each scan contains a timestamp data which is onsource-data
- A polynomial is fitted [4] across the phase part of this onsource data over all channels.

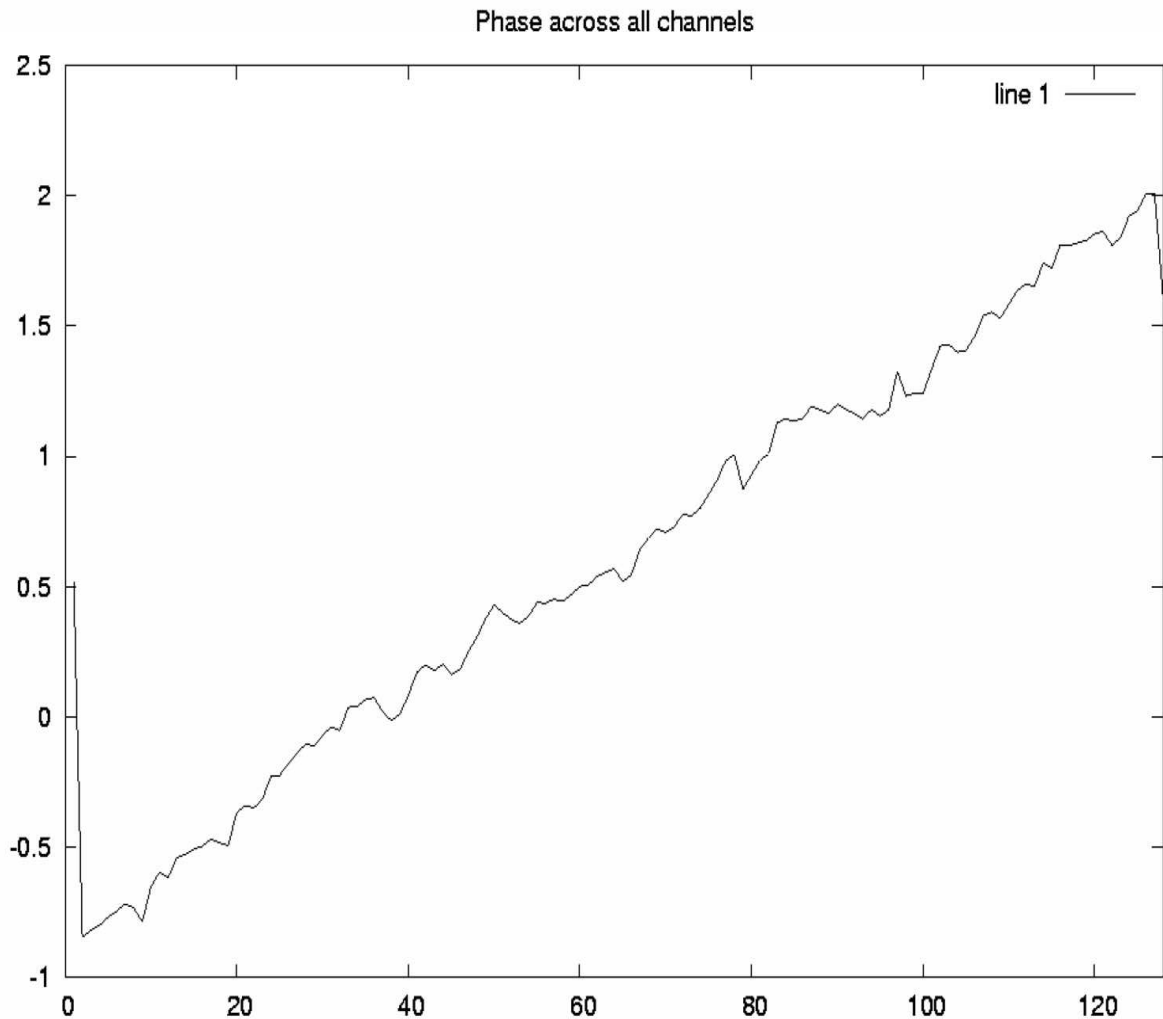


Figure 5.2: Variation of phase across all channels at 130

- Then this fit is subtracted from the actual onsource data \Rightarrow '*calibdata*'
- Now this '*calibdata*' is subtracted from all the other timestamp data for each individual channels (in phase only)
- Now we simply take the mean of all the channels for each timestamps, where the amplitude part is simply averaged while the phase part is averaged after the **BandPass Calibration** has been done

5.3 Smoothing the Data

After averaging the data over all channels, we have now all 19 scans having 1 data per timestamp. But even after channel collapse we observe that the

data contains effects of the RFI and Interplanetary scintillations. So in order to eliminate these effects we had to smooth the data.

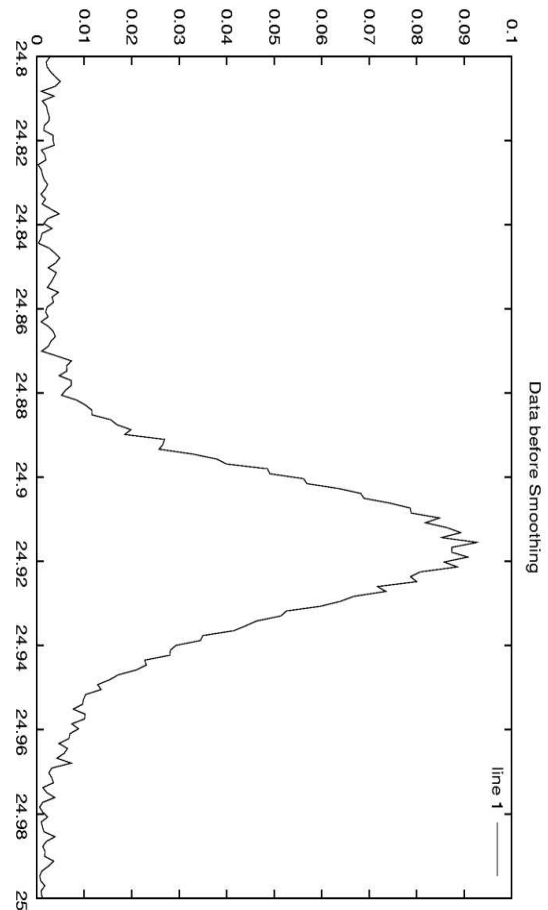


Figure 5.3: Scan data with RFI and scintillations

The Fast Fourier Transform was used in order to transform the data from the time domain to the frequency domain. We know that the radio sources across the sky has a radiation pattern which will much slowly varying as compared to the RFI(Radio Frequency Interference) or Scintillations (mostly Ionospheric). So after taking the FFT(Fast Fourier Transform) we saw that there is response at the higher side of the frequency domain which was identified to be due to RFI or scintillations. So we padded the frequency domain data with zeros on the higher side of the frequency domain down to a limit so that we do not lose on the actual data. And then the IFFT(Inverse Fourier Transform) of this padded data has been taken. The result of this process gave us a much smoother data free from the RFI and Scintillations upto an appreciable amount.

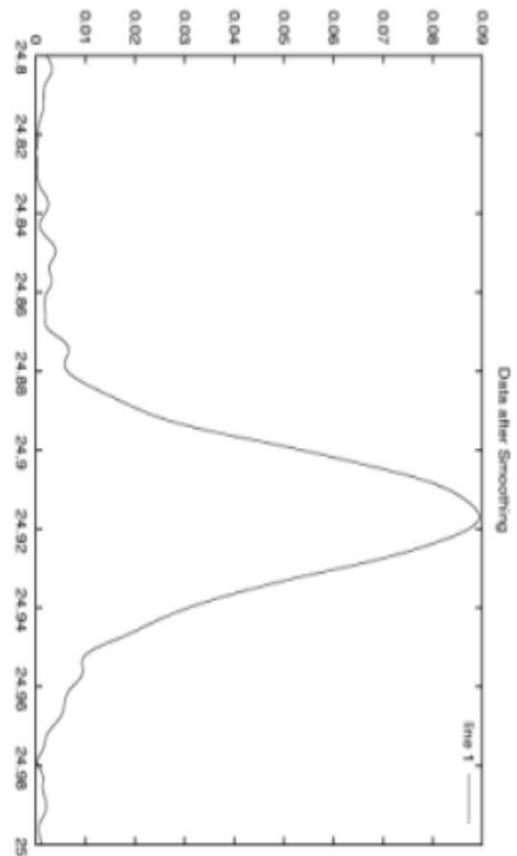


Figure 5.4: Scan-data after smoothing out the RFI and Scintillations

5.4 Transforming from Far Field to Aperture Field

Now we are left up with the job of assembling all the scans on the skyplane and transforming it back to the aperture plane.

In order to assemble all the scans together in the sky-plane data for each scan is normalised in amplitude with respect to the onsource data and the phase of the onsource data is subtracted from all the other data

This is done to calibrate all the scans such that the value of onsource data should be the same in all the scans(which should have been ideally the case). Direct Fourier Transform Relation is used in order to get the Aperture-field

Distribution on the dish.

$$\tilde{E}(x, y) = \int \int E(\theta_x, \theta_y) e^{i2\pi(\theta_x x + \theta_y y)} d\theta_x d\theta_y \quad (5.1)$$

The form of the above continuum relation that is used in the algorithm is [3]:

$$\tilde{E}(x, y) = \sum_{\theta_x, \theta_y} E(\theta_x, \theta_y) e^{i2\pi(\theta_x x + \theta_y y)} \quad (5.2)$$

where

θ_x and θ_y are sky-plane coordinates and x, y are coordinates on dish.

The corresponding 2 dimensional Discrete Fourier Transform is given by:

$$A(p, q) = \sum_m \sum_n A(m, n) e^{j2\pi(\frac{pm+qn}{N})} \quad (5.3)$$

where

$$\frac{x.\theta}{\lambda} = \frac{n.p}{N} \text{ and } \frac{y.\phi}{\lambda} = \frac{q.m}{N}$$

$$\Delta x . \Delta \theta = \frac{\lambda}{N}$$

Chapter 6

Results and Measurement of Surface Errors

This chapter deals with the results that are obtained from the observation mentioned in Chapter 4. Here the calculation of the surface errors over the dish is also mentioned.

6.1 Measurement of Surface Errors - Theory

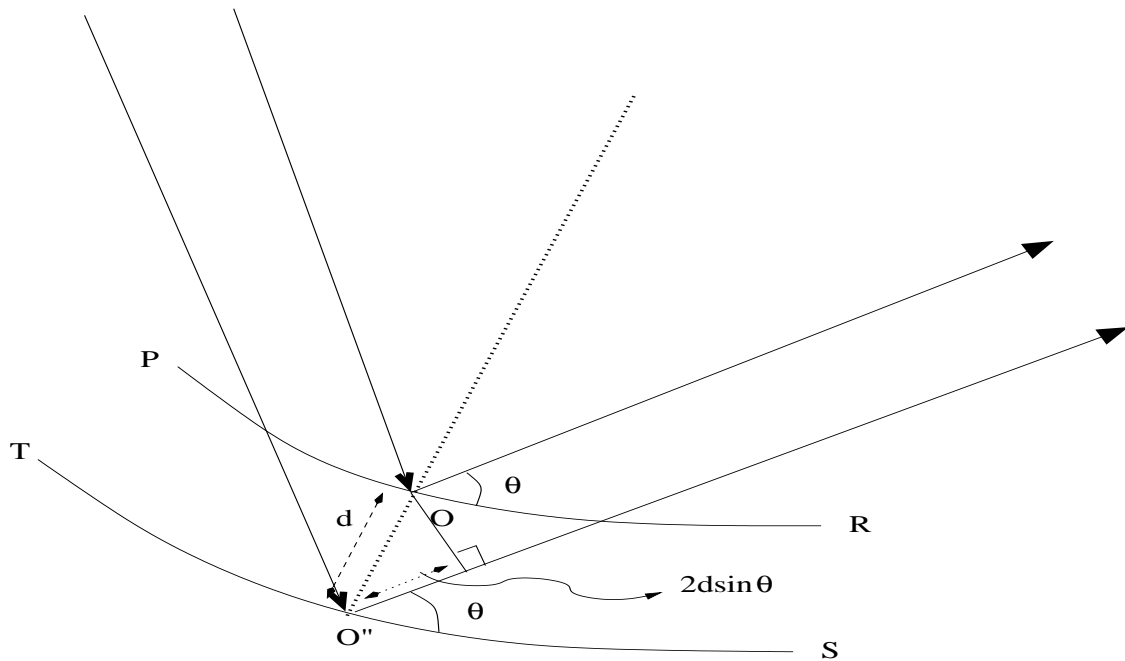


Figure 6.1: Diagram illustrating the effect of the distortion of the surface of the dish

In order to calculate the surface errors in several antennas we refer to figure 6.1 . In the figure surface $\vec{P\ddot{O}R}$ represents the original undistorted surface of

any antenna. And the surface $T\vec{O}''S$ represents the distorted surface. Let us take the shift in the surface i.e. $O\vec{O}''$ to be of the value 'd' which is in the direction normal to the original surface $P\vec{O}R$. Now from the figure 6.1 we can make out that the path difference introduced due to the surface error of 'd' is $2d\sin\theta$. So we get the phase difference introduced across the surface due to this deformation of 'd' as given by :

$$\Delta\phi = \frac{2\pi}{\lambda}2d\sin\theta \quad (6.1)$$

Since in our case the frequency of observation is 1280 MHz, it gives the wavelength $\lambda = 23.44\text{cm}$. And if we consider $\theta = 90^\circ$ i.e. for normal incidence of the radio-waves on the surface of the reflector(which occurs for the inner part of the dish), then we get approximately the phase change as :

$$\Delta\phi = \frac{4\pi d}{\lambda} \quad (6.2)$$

This result relates that if in the phase contour of each antenna we observe a phase change of 1 radian then it is related to a surface error of 1.87 cm.

Now it is clear from the Figure 6.1 that if the surface of the dish is distorted in the downward direction then the corresponding phase change will be positive, and when the distortion is upward from the surface of the dish, then the corresponding phase change will be negative

So in the above case the phase variation of +1 radians across the surface indicates that over that region the surface might have been pushed down by an amount of 1.87 cm , while a phase change of -1 radian indicates that in that region there might be a upliftment of the surface by an amount of 1.87 cm.

6.2 Image of Dish

In this section we present the contour plots of different antennas in both 130 and 175 polarisations. The contour plots are separate for Phase and Amplitude parts.

Here we digress a bit to explain the meaning of the terms 130 and 175. The data that are collected at each antenna are sent to the Central Electronics Building from the Antenna Base through the optical fibres. Now, the antennas can record the data at two different polarisations at each frequencies (Right Circular Polarisation and Left Circular Polarisation). So the data of both these polarisation data are sent simultaneously through the optical fibres using two different frequencies 130 and 175 MHz. Its noteworthy here that at L Band we dont have the LCP and RCP but 2 linear polarisations

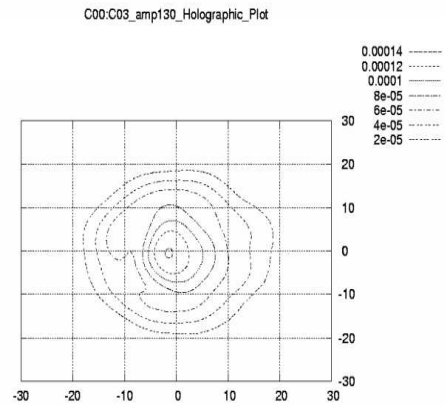
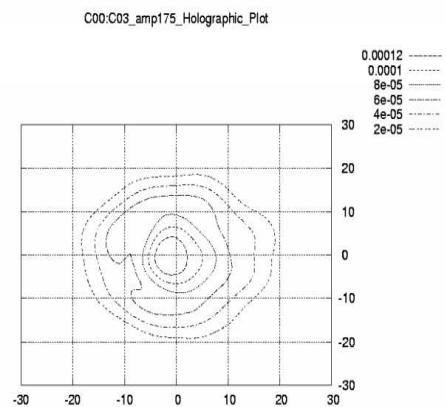


Figure 6.2: Amplitude At 130 and 175 for C03 in reference to C00



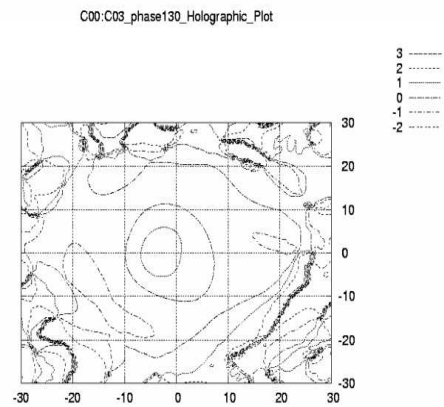
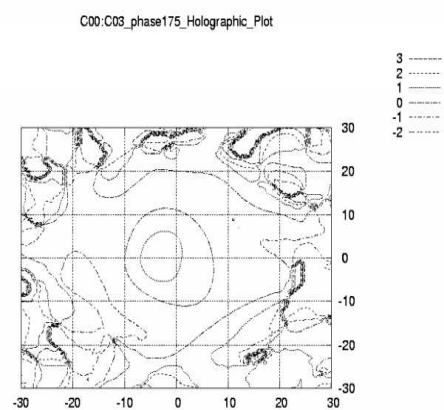


Figure 6.4: Phase At 130 and 175 for C03 in reference to C00



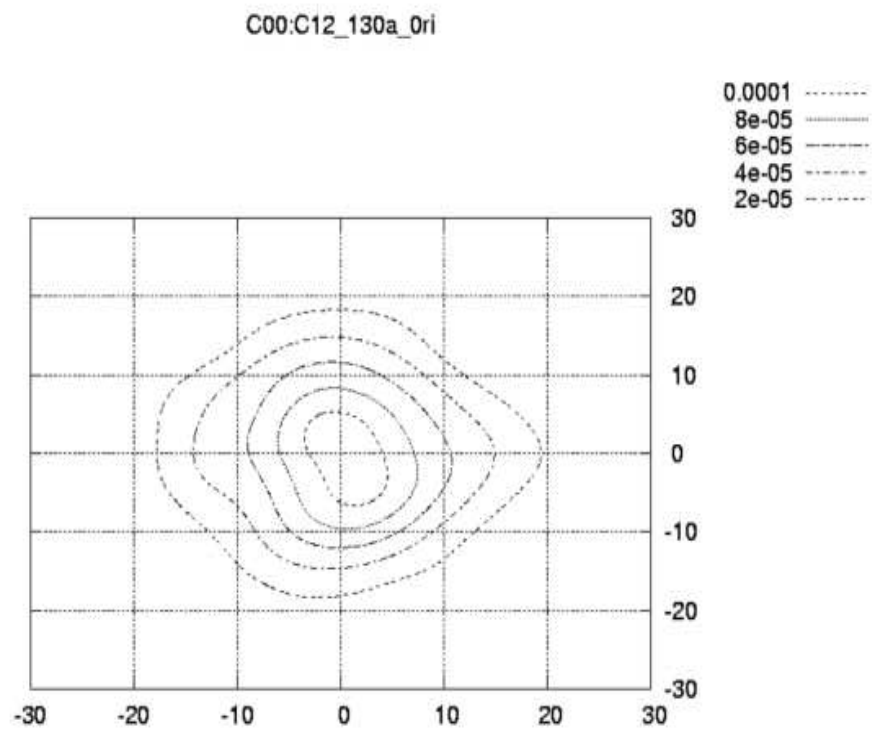
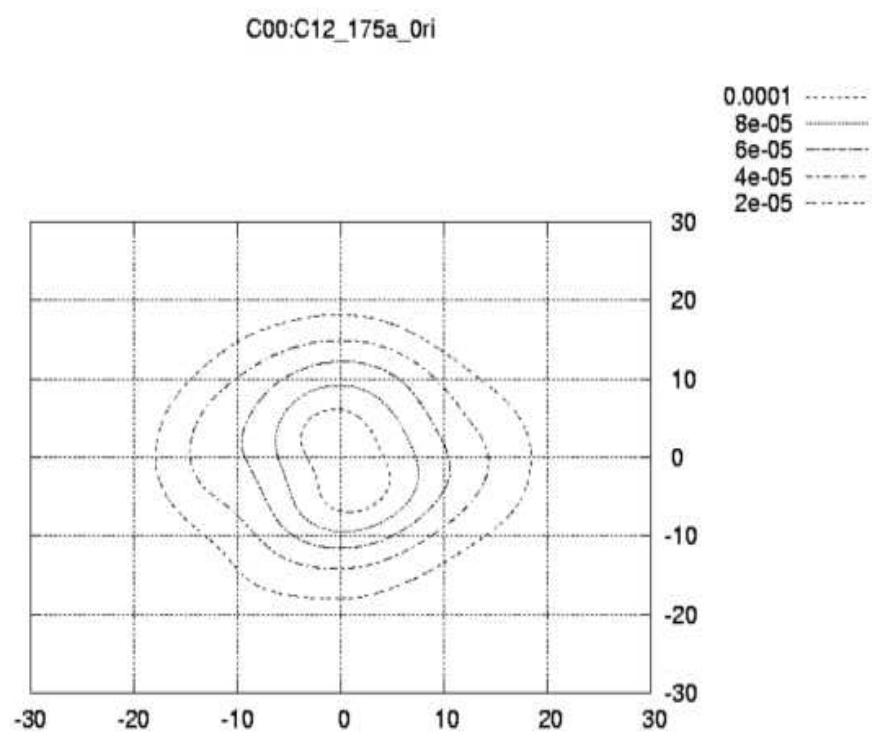


Figure 6.6: Amplitude At 130 and 175 for C12 in reference to C00



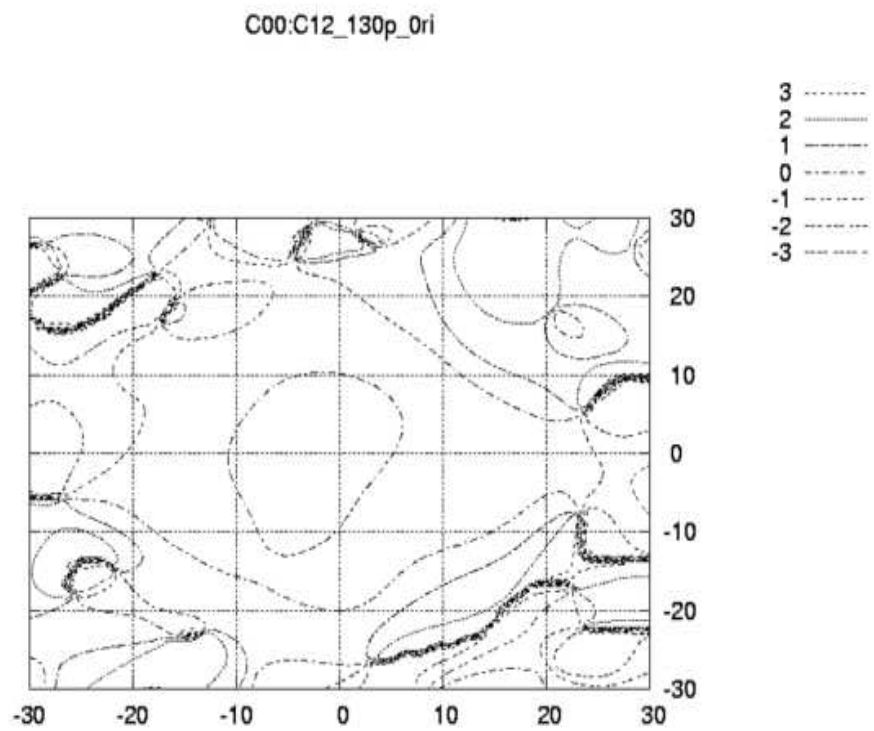
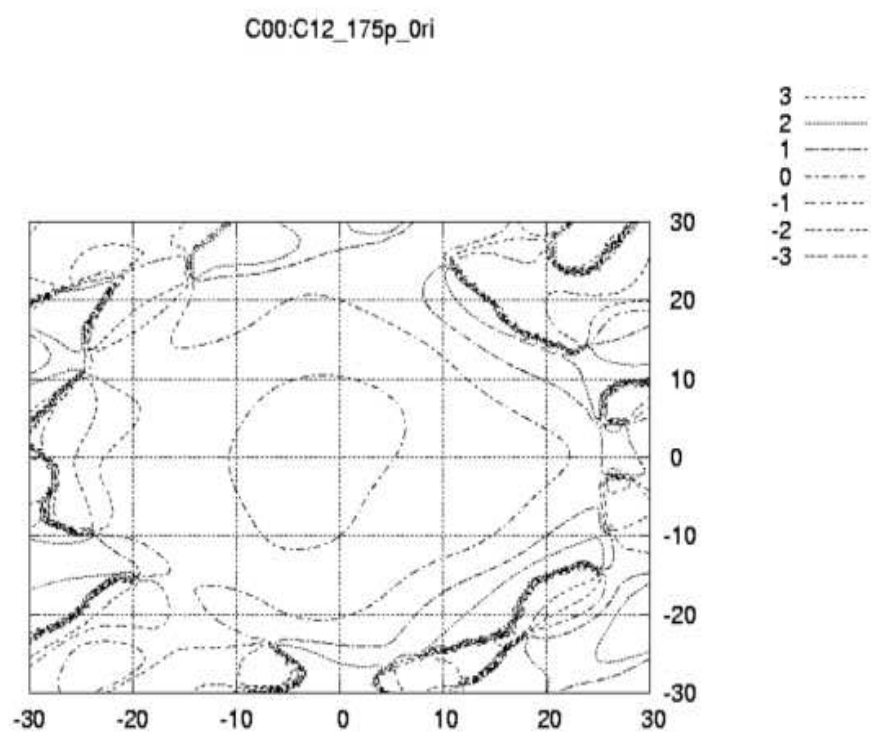


Figure 6.8: Phase At 130 and 175 for C12 in reference to C00



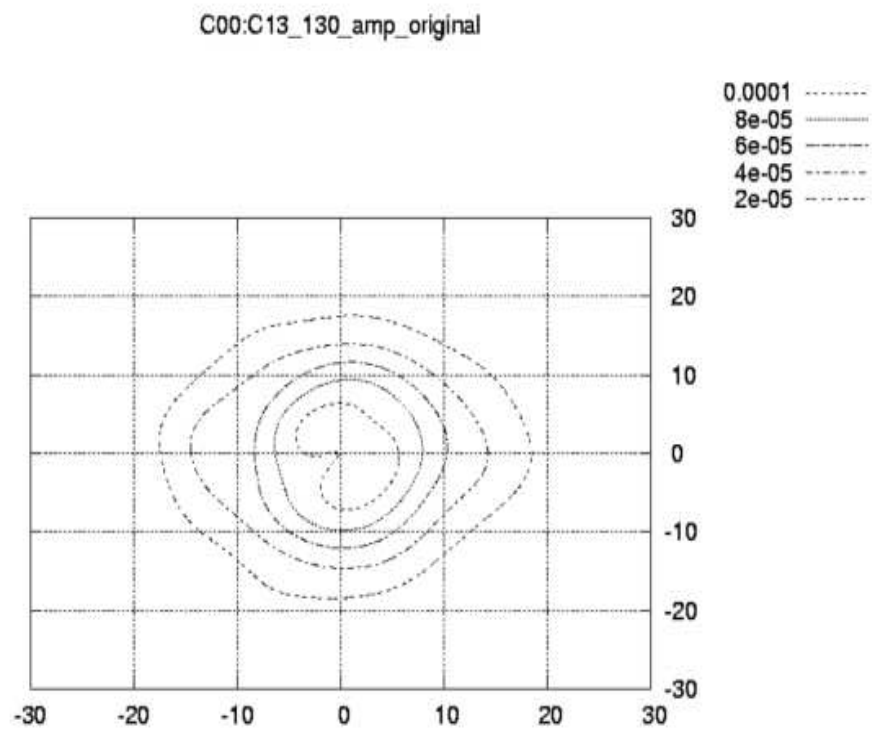
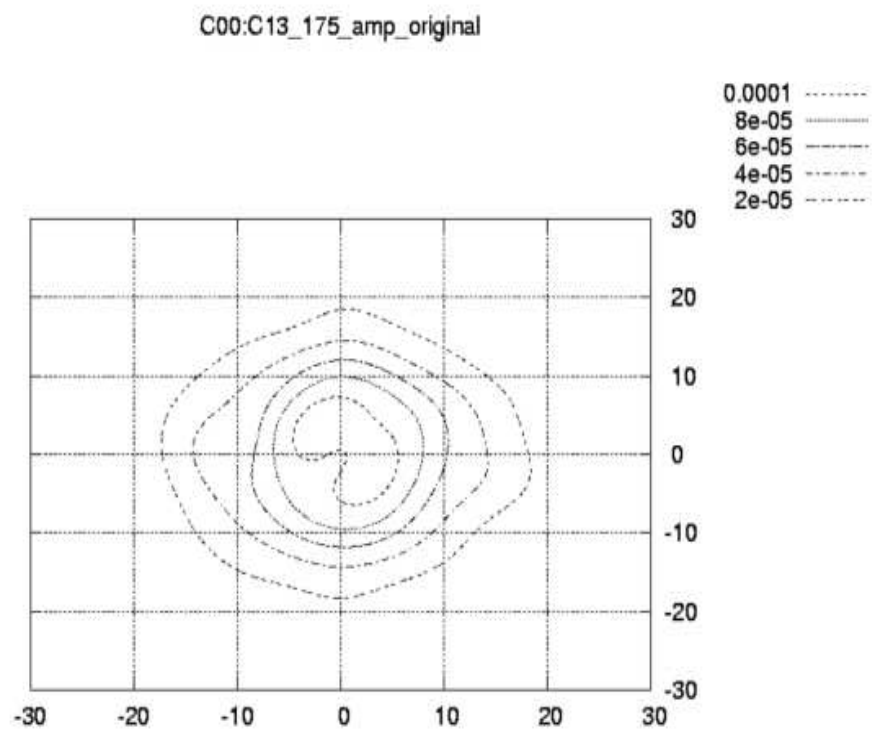


Figure 6.10: Amplitude At 130 and 175 for C13 in reference to C00



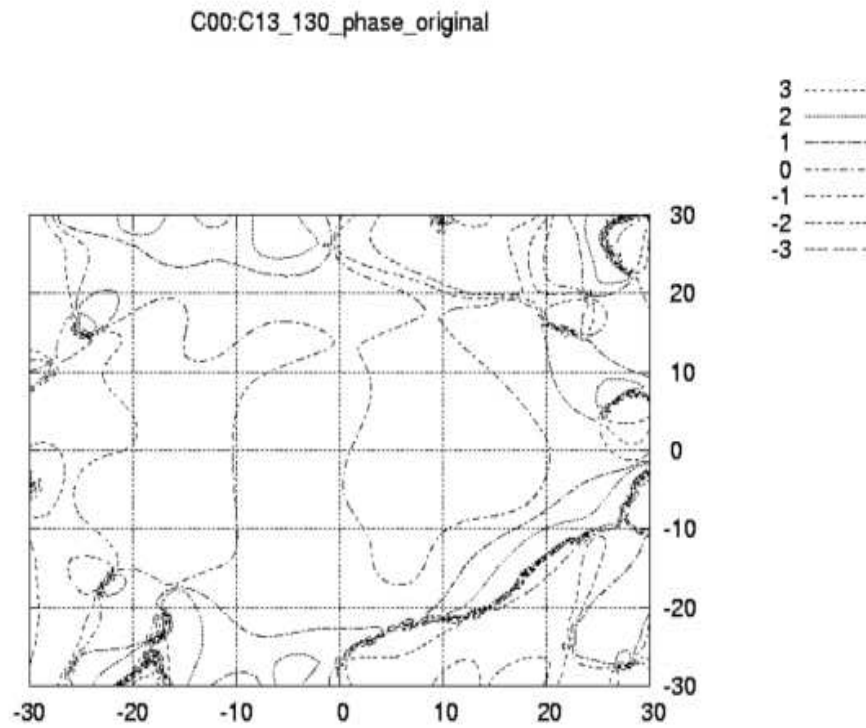
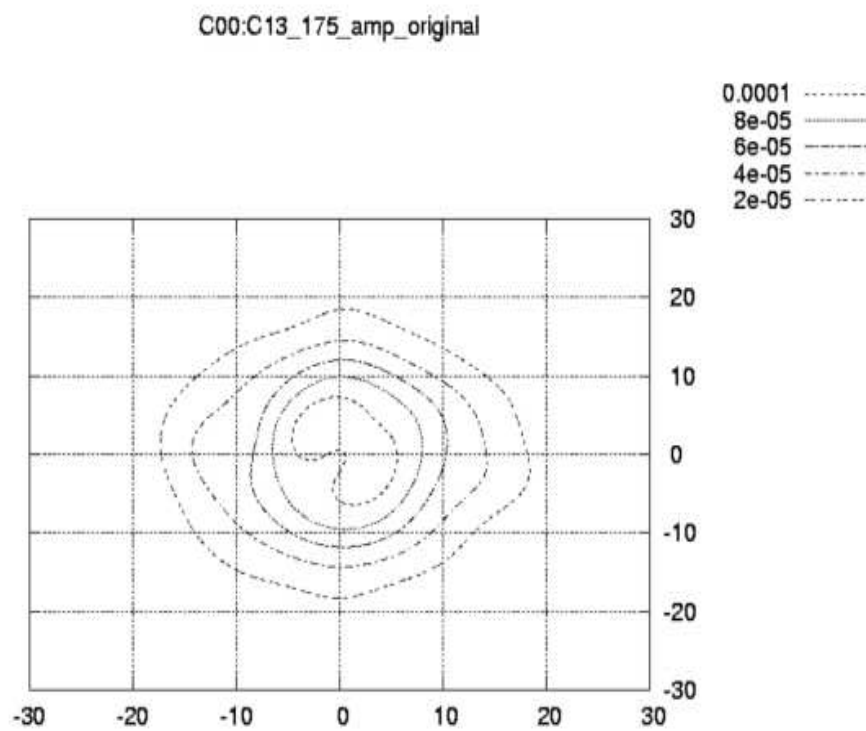


Figure 6.12: Phase At 130 and 175 for C13 in reference to C00



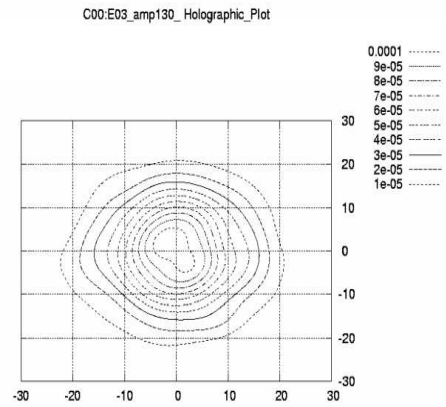
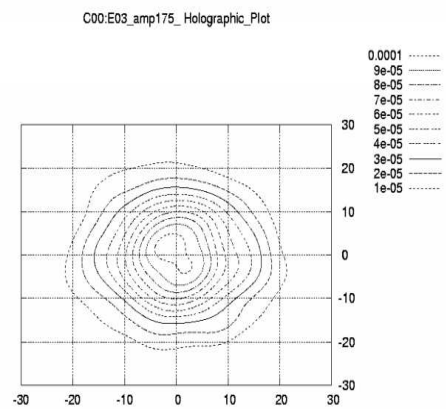


Figure 6.14: Amplitude At 130 and 175 for E03 in reference to C00



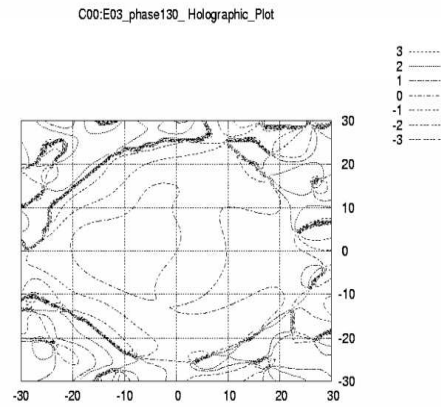
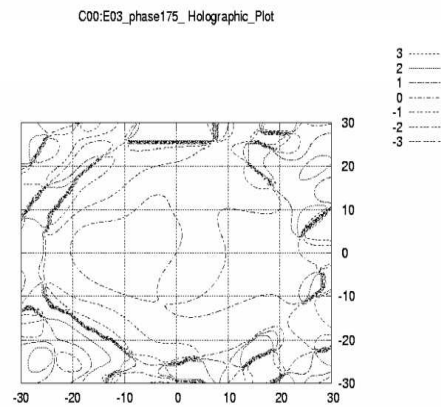


Figure 6.16: Phase At 130 and 175 for E03 in reference to C00



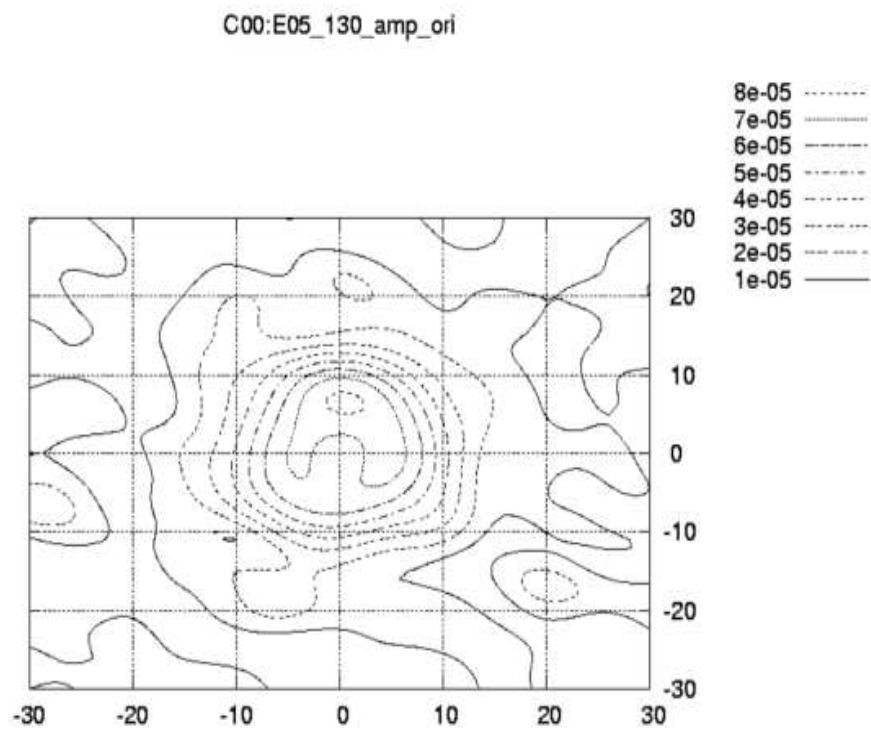
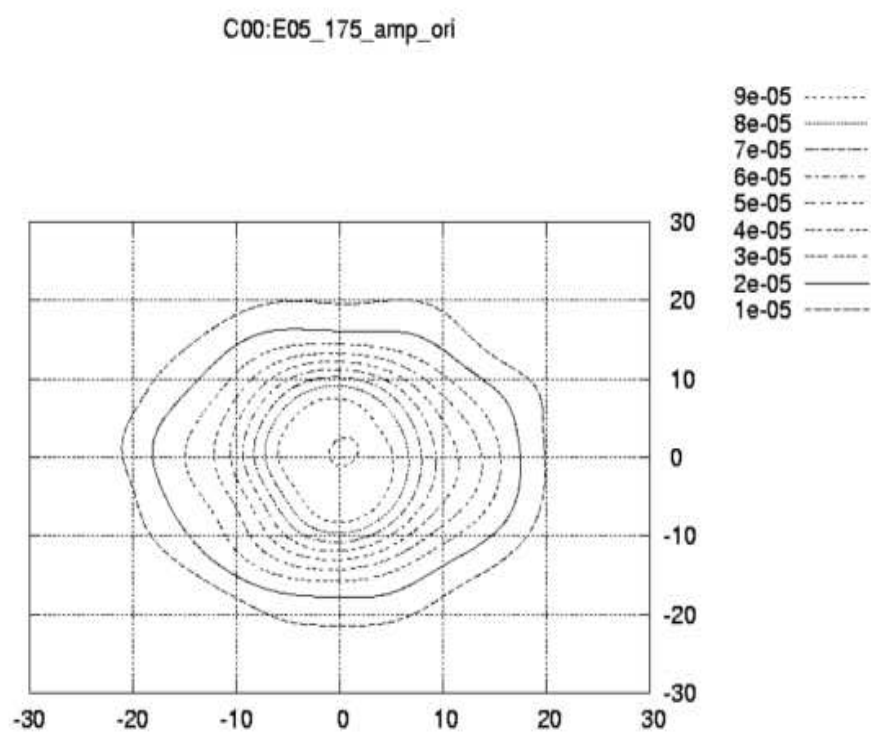


Figure 6.18: Amplitude At 130 and 175 for E05 in reference to C00



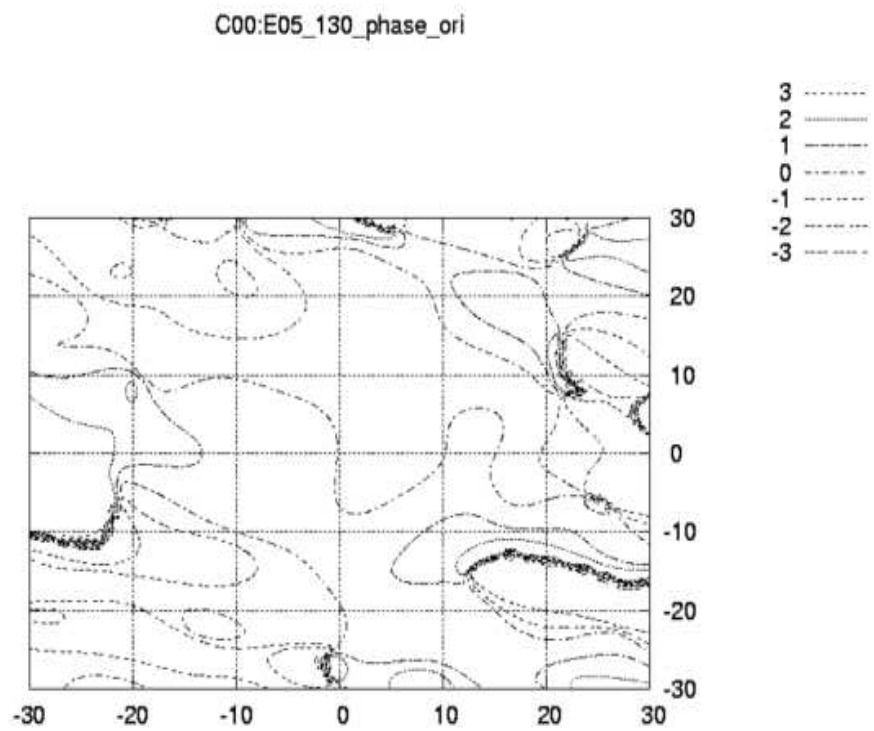
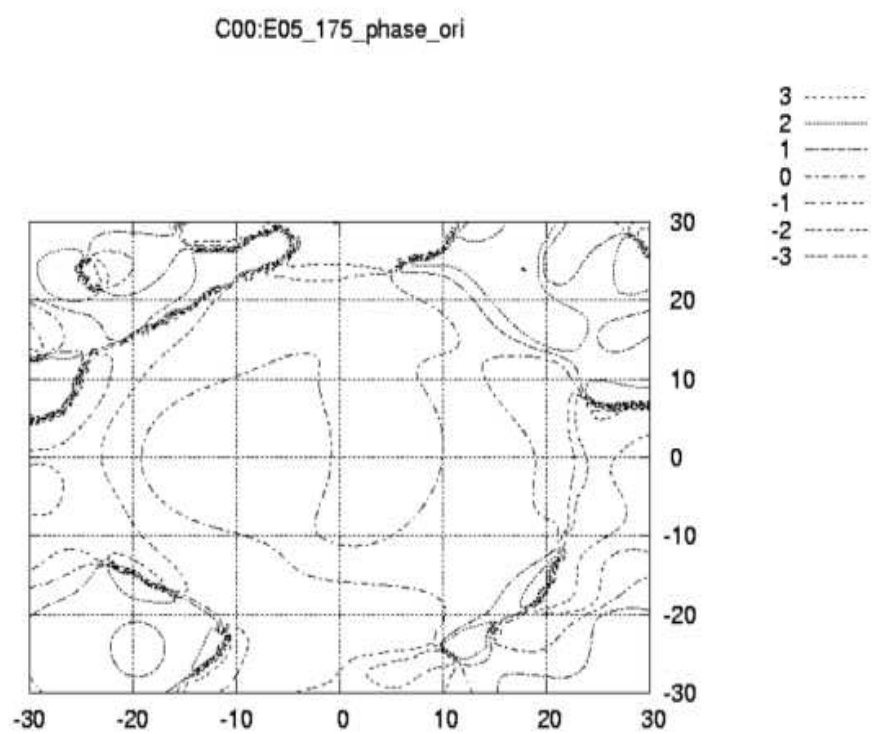


Figure 6.20: Phase At 130 and 175 for E05 in reference to C00



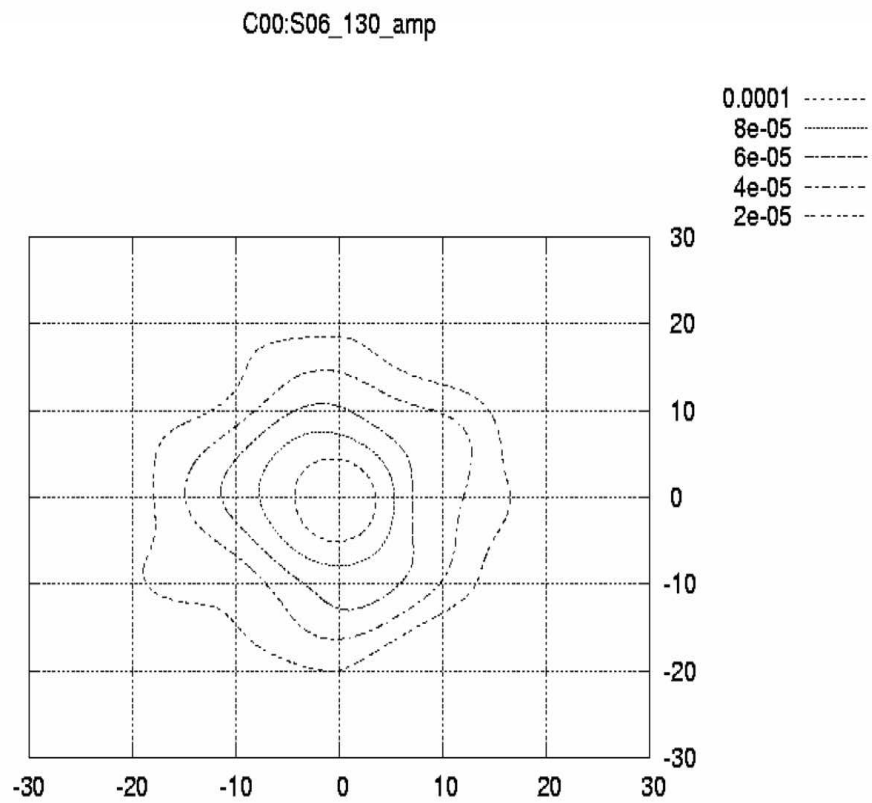
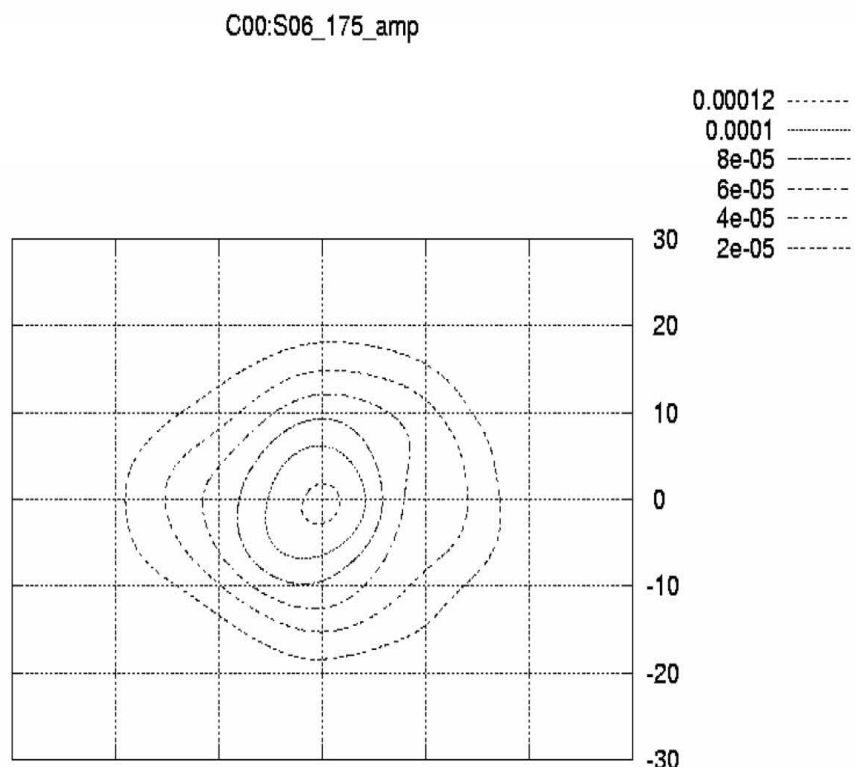


Figure 6.22: Amplitude At 130 and 175 for S06 in reference to C00



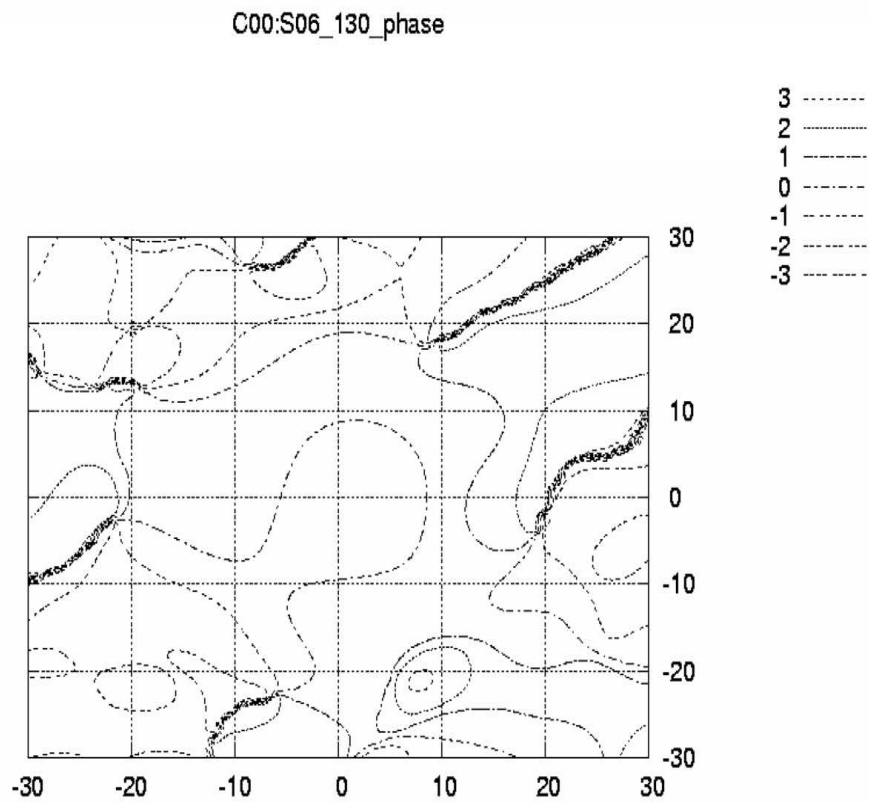
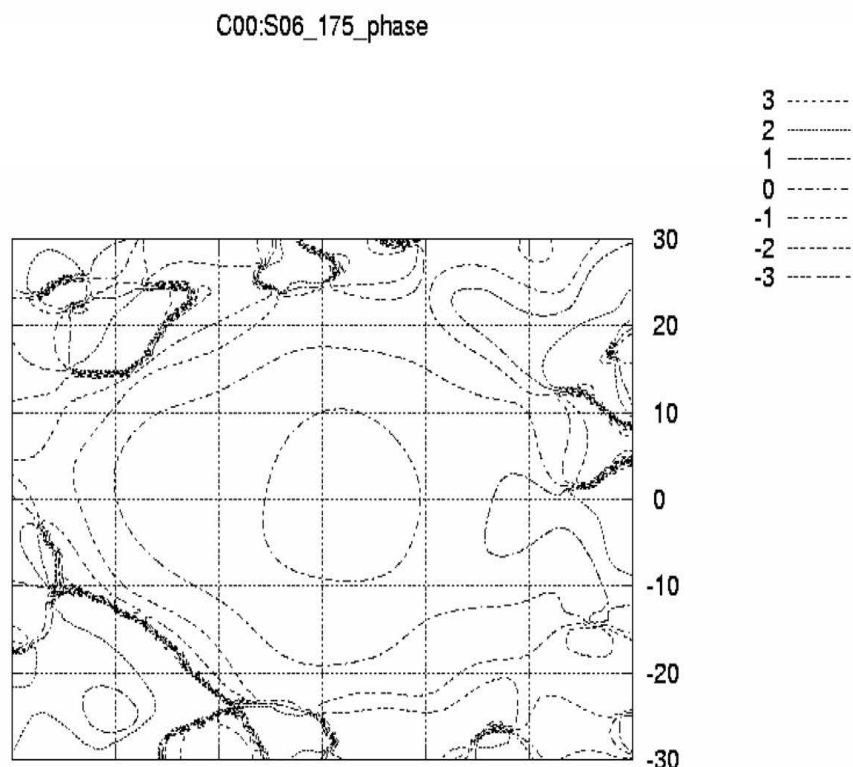


Figure 6.24: Phase At 130 and 175 for S06 in reference to C00



6.3 Self-Consistency Checks

6.3.1 Theory

At this point we have data of each target antennas for two reference antennas. So we can actually check the consistency between the results of each antenna when corelated with two refernce antennas (for each polarisations).

We follow a following technique to determine the same:

Let the aperture field distribution of a antenna due to 1st reference antenna is $E^{(1)}(x, y)$ and that due to the 2nd be $E^{(2)}(x, y)$, then the relation giving percentage of consistency is given as:

$$\gamma = \frac{\int_{entiredish} |E^{(1)}(x, y) - E^{(2)}(x, y)|^2 dx dy}{\sqrt{\int |E^{(1)}(x, y)|^2 dx dy \int |E^{(2)}(x, y)|^2 dx dy}} \times 100\% \quad (6.3)$$

Now, if we are going to check for one antenna and the same reference but the self-consistency between polarisation, then $E^{(1)}(x, y)$ and $E^{(2)}(x, y)$ are respectively the fields due to each of 130 and 175 polarisations.

6.3.2 Results for C03

The self-consistency between two referrences C10 and C00 at 130 is about 3.4% and that at 175 is 3.5%.

The self-consistency between two polarisations of C03 with reference C00 is given by 0.39%

Chapter 7

Measurement of Defocus

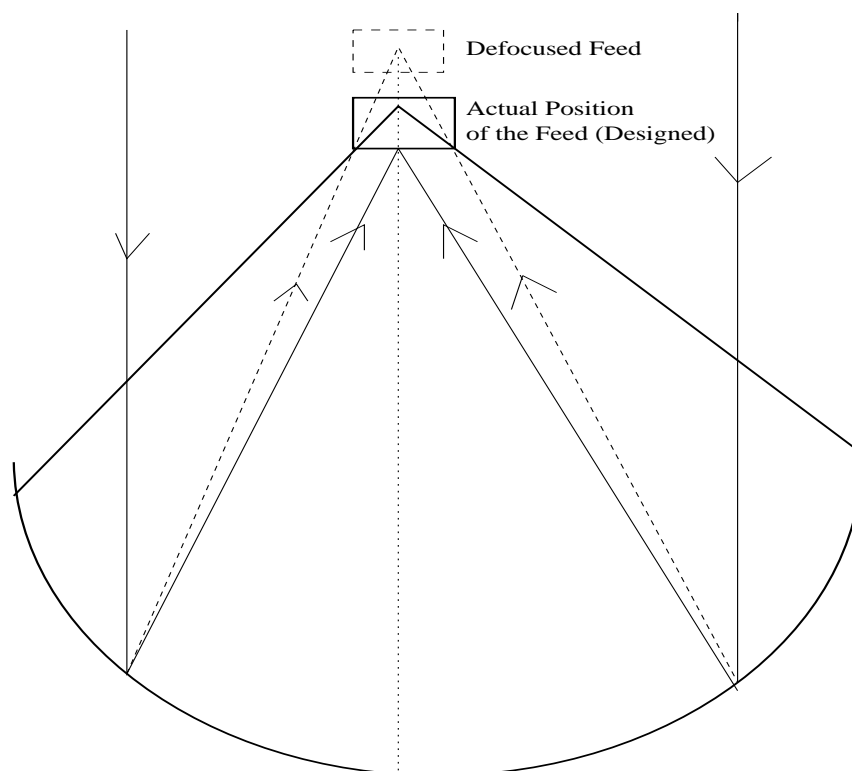


Fig: Showing Defocus of the Feed

Figure 7.1: Diagram depicting the condition after the defocus of the feed

This chapter deals with the measurement of the defocus of the feed in separate antennas due to the feed displacement.

7.1 Theory for measuring the defocus

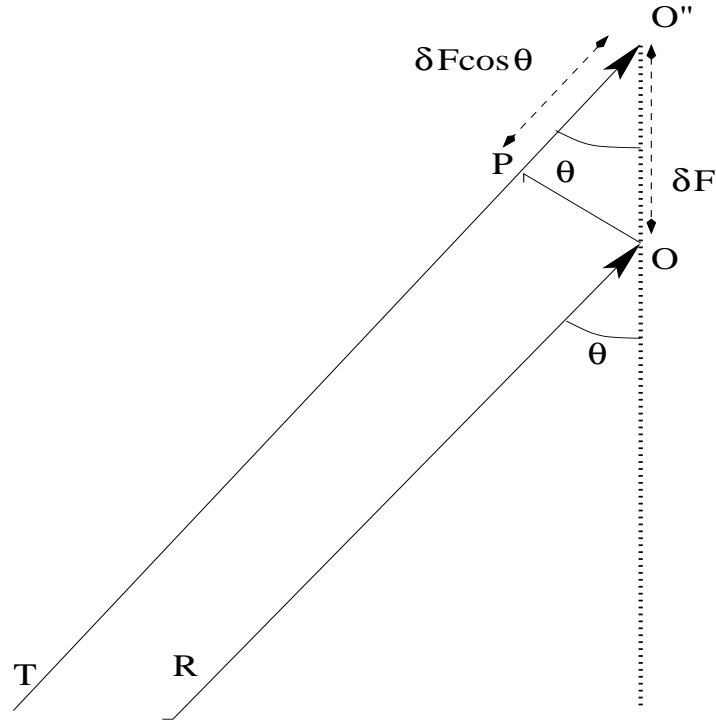


Figure 7.2: Diagram illustrating the effect of the defocus of the feed

From the figure 7.2 it is certain that the path difference δL introduced due to the defocus of the feed by the extent of δf is given by:

$$\delta L = \delta f(1 - \cos \theta) \quad (7.1)$$

In the above equation the actual path difference remains as $\delta f \cos \theta$, but in addition of a constant term δf does not change the information.

For small values of θ we can approximate the above equation as

$$\delta L = \delta f \frac{\theta^2}{2} \quad (7.2)$$

Now, since $\theta = R/f$ where $R = \sqrt{x^2 + y^2}$ = distance of different mesh points on the dish, and f = focal length

$$\therefore \delta L = \delta f \frac{x^2 + y^2}{2f^2} \quad (7.3)$$

So the corresponding phase difference $\delta \phi$ introduced on the surface of the dish due to the defocus of the feed is given by :

$$\delta \phi = \delta f \frac{x^2 + y^2}{2f^2} \frac{2\pi}{\lambda} \quad (7.4)$$

where λ is the wavelength of observation

7.2 Analysis

We have taken the phase part of the holographic data for each antenna at both 130 and 175 polarisations and has extracted a quadratic function from it in the following way.

$$\mathcal{R} = \sum_{\sqrt{x^2+y^2} < R_{max}} (\text{phase}(x, y) - \alpha(x^2 + y^2))^2 \quad (7.5)$$

where R_{max} denotes the extent (in radius) of the dish to be taken into consideration while doing this computation. Here we have taken R_{max} to be 15 meters.

the array phase(x,y) denotes for each of 130 and 175 polarisations. So here we have calculated the value of \mathcal{R} for 130 and 175 separately.

α is the parameter we have used to get the minimum value of \mathcal{R} .

So by varying the value of α we have obtained the minimum value of \mathcal{R} . This value of α corresponding to the minimum value of \mathcal{R} we have compared with the above theory to get the value of defocus of the feed for a particular antenna. It is important to mention here that the value of α at minimum value of \mathcal{R} is almost same for both 130 and 175.

$$\alpha = \frac{2\pi\delta f}{2f^2\lambda} \quad (7.6)$$

$$\therefore \delta f = \frac{\alpha\lambda f^2}{\pi} \quad (7.7)$$

7.3 Results for C03

Taking Focal Length = 18.54 meters, Wavelength of Observation = 0.23438 meters (at 1280 MHz), and value of α from the minimisation procedure we get the value of the defocus $\delta f = 0.17951$ meters both at 130 as well as 175 polarisations. This measure of defocus is about 0.97% of the total focal length.

Chapter 8

Holography at 610 MHz

Till now the results of holographic measurement at 1280 MHz has been mentioned. In order to validate the holographic procedure followed there have been a need to check the results at 610 MHz also. Ideally it should give similar results to those obtained at 1280 MHz. As compared to the L-band feed (a corrugated horn) of GMRT the 610 feed is a coaxial cylinder having the dual frequency mode at 610 MHz and also at 327 Mhz.

8.1 Scanning Technique

The technique is identical to that mentioned in chapter 4 (in case of 1280 MHz). But primary beamwidth at 610 MHz is 54 min. So to perform the entire observation of 19 scans(6 beamwidths each) in short time the scan rate was taken to be 36 arcmin per min as compared to 18 arcmin per min in case of 1280 MHz. In this observation the source was 3C147 (as in chapter 4).

In this observation, different antennas were given different magnitude of feed rotations in either anticlockwise or clockwise directions. But still some of the antennas (including the reference antennas were kept at pointing only and not been given any pointing offset. This action of feed rotation will introduce deliberately a coma term in the phase distribution across the surface of the dish.

The status of the feed-rotation in each antennas used is given as follows:-

- C01,C10(Reference Antennas)→ no feed-rotation.
- C02,C03,C04,C05,C11,E03,E04,E06 → no feed-rotation.
- S03,S06 → feed rotated by +200 counts.
- E02,E05 → feed rotated by -200 counts.
- C09,W03 → feed rotated by +300 counts.
- S01,W02 → feed rotated by -300 counts.

- C12,C13 → feed rotated by +400 counts.
- C08,W01 → feed rotated by -400 counts.

Here, we should mention that Feeds at GMRT are controlled by the FPS(Feed Positioning System) and the convention used by FPS for rotation is 15360 counts 270° . And +,- sign resembles the clockwise and anticlockwise rotations respectively.

8.2 Results

Presently only one antenna(E03) at 610 MHz has been analyzed in reference to C01.

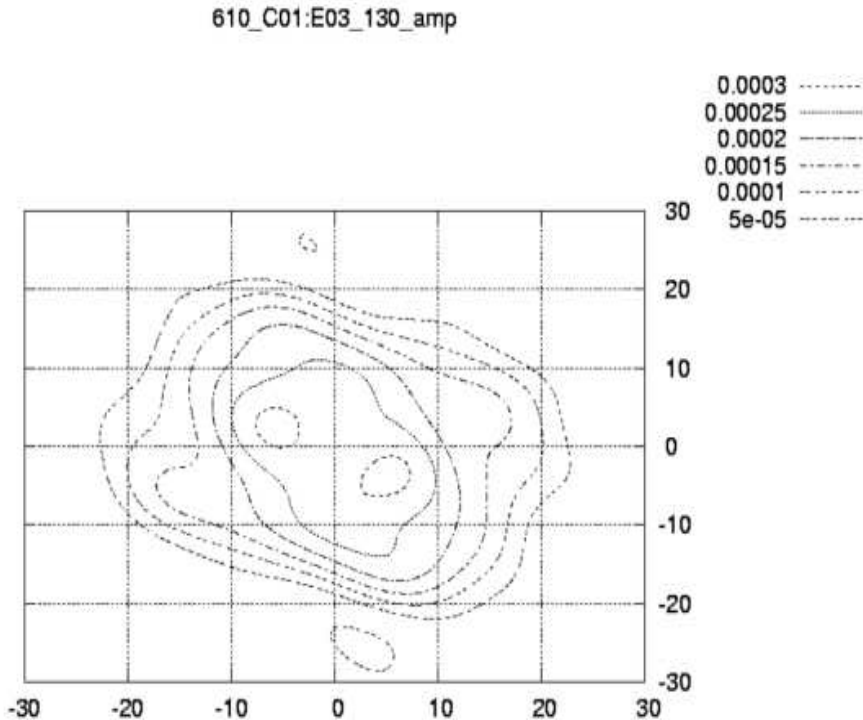
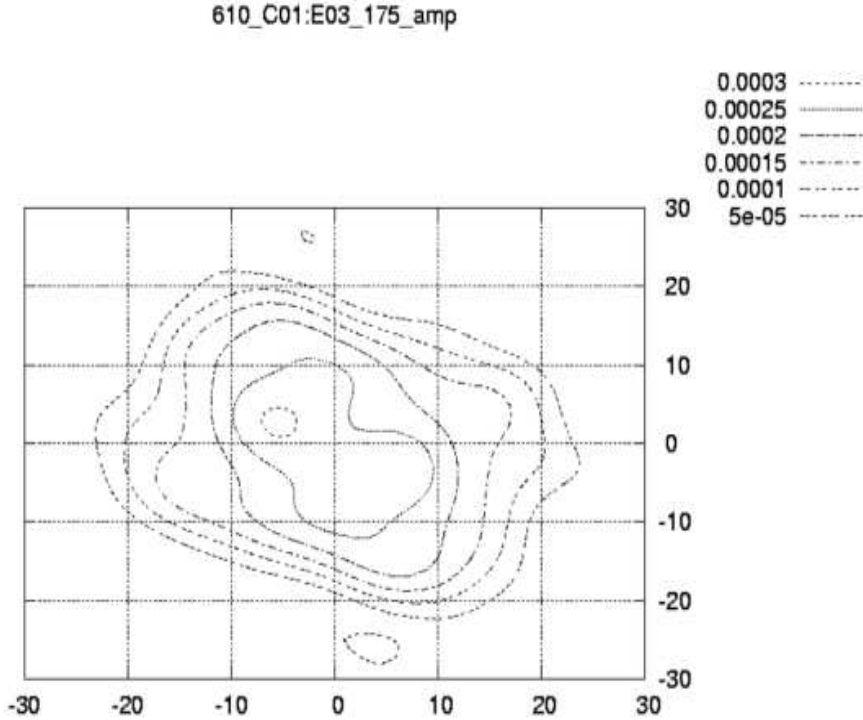


Figure 8.1: Amplitude At 130 and 175 for E03 with reference as C01



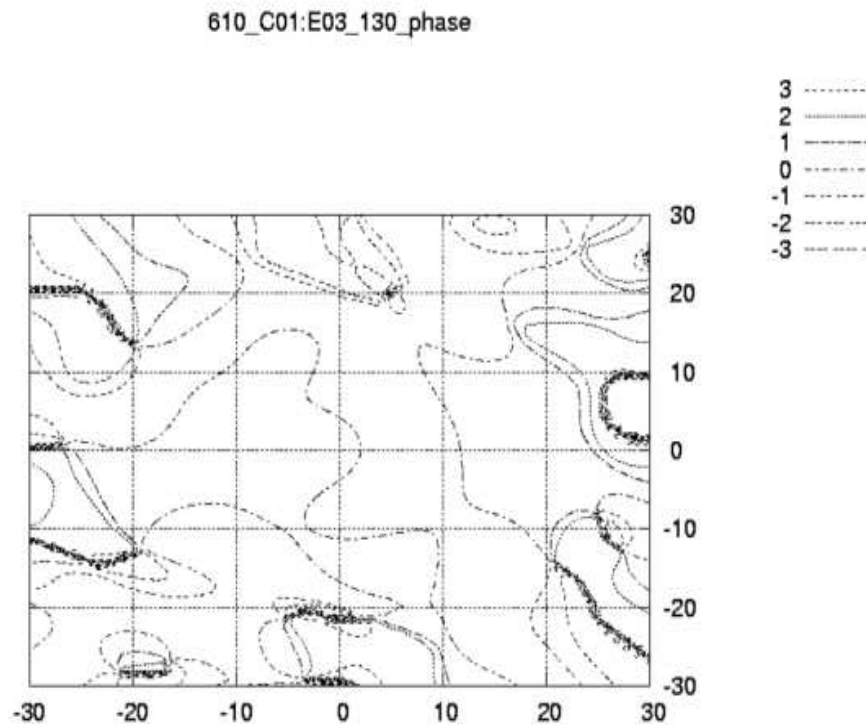
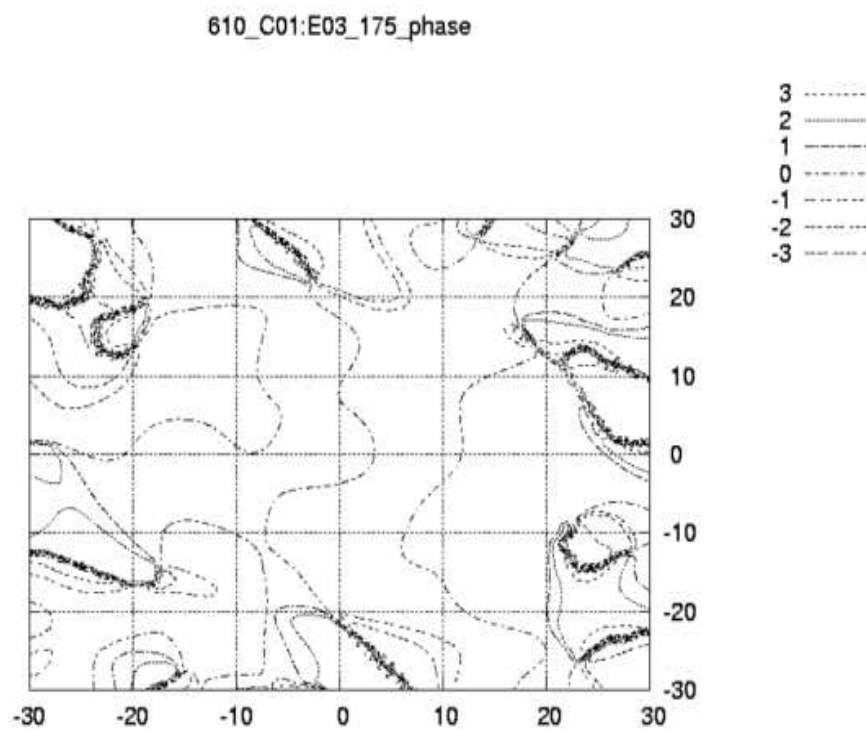


Figure 8.3: Phase At 130 and 175 for E03 with reference as C01



Chapter 9

Second Observation at 1280 MHz

There was a need of the second observation at 1280 MHz in order to justify the consistency of the results of last observation at 1280 MHz(mentioned in Chapter 4.

9.1 Scanning Technique

The technique is exactly the same as mentioned in chapter 4. But tis time the entire observation of 19 scans(6 beamwidths each) was to be peformed in short time, so the scan rate was taken to be 36 arcmin per min as compared to 18 arcmin per min in chapter 4. In this observation the source was 3C286.

In this observation, different antennas were given different magnitude of feed rotations in either anticlockwise or clockwise directions. But still some of the antennas (including the reference antennas were kept at pointing only and not been given any pointing offset. This action of feed rotation will introduce deliberately a coma term in the phase distribution across the surface of the dish.

The status of the feed-rotation in each antennas used is given as follows:-

- C00,C06,C10(Reference Antennas)→ no feed-rotation.
- C01,C02,C03,C04,C05,E03,S04,W06 → no feed-rotation.
- C05,E06,S06 → feed rotated by +200 counts.
- E05,S03,W04 → feed rotated by -200 counts.
- E02,E04,W03 → feed rotated by +300 counts.
- C14,S01,W02 → feed rotated by -300 counts.
- C12,C13,W01 → feed rotated by +400 counts.
- C08,C09,C11 → feed rotated by -400 counts.

9.2 Results

In the next figures, we can see the results of C03(with reference to C00). The observed pattern is similar to that obtained chapter 6. In fact, the consistency calculationas per equation 6.3 gives 4.9% at 130 and 5.1% at 175.

9.3 Estimate of Coma

The qualitative behaviour of coma has been observed in the above sets of data. The behaviour is at per with the expected as referred in [6]. We are trying to extract the quantitative measure of Coma as well.

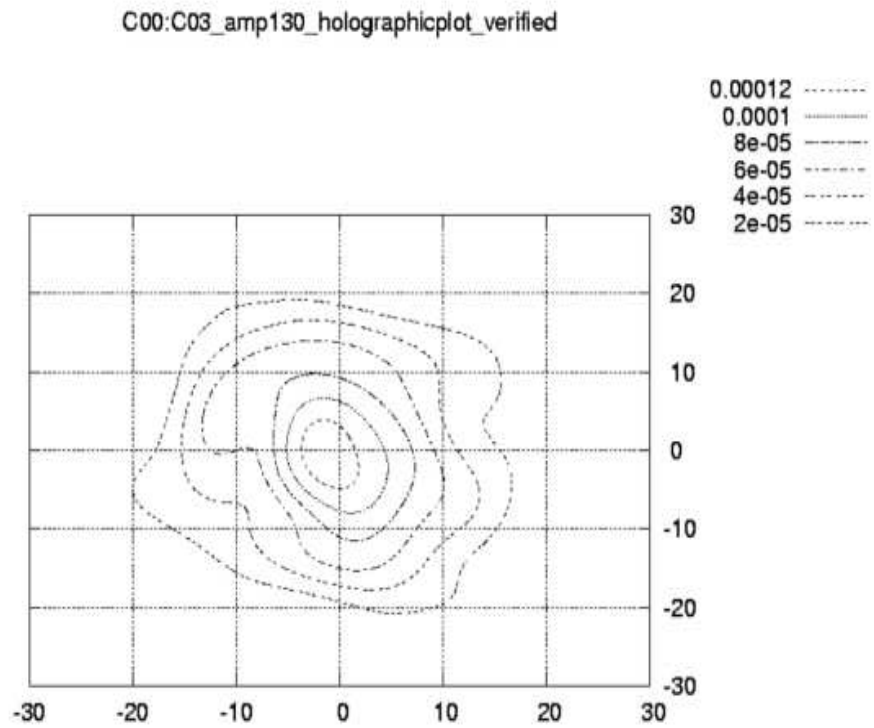
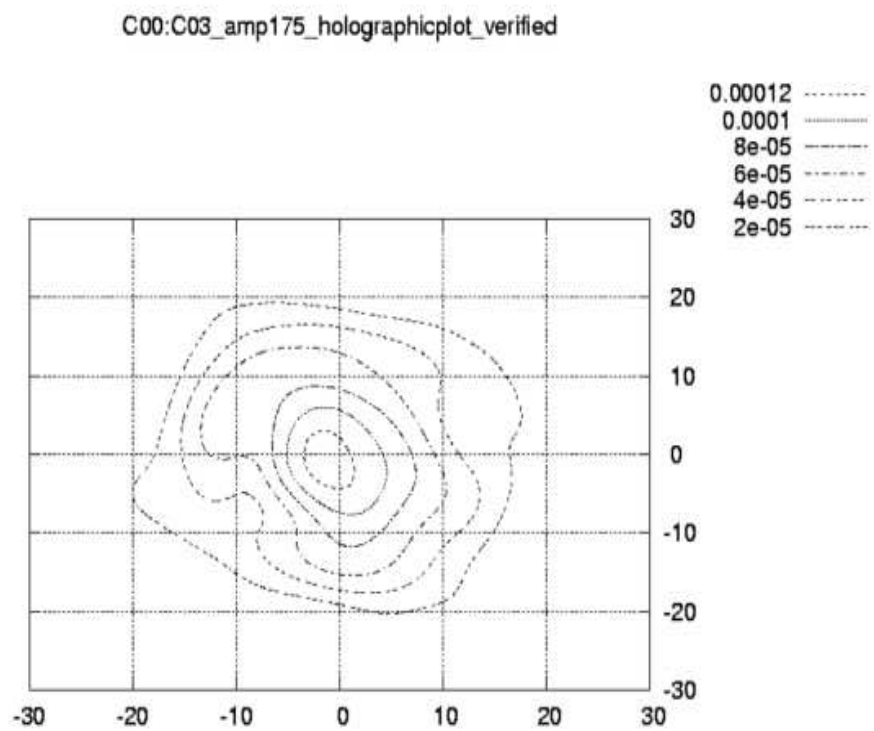


Figure 9.1: Amplitude At 130 and 175 for C03 with reference as C00 without feed rotation



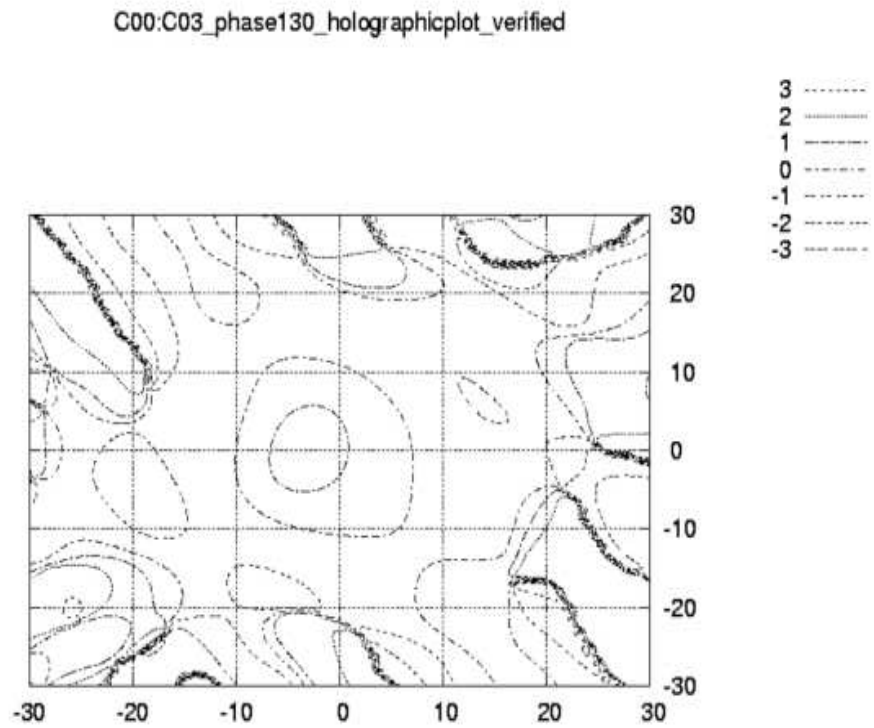
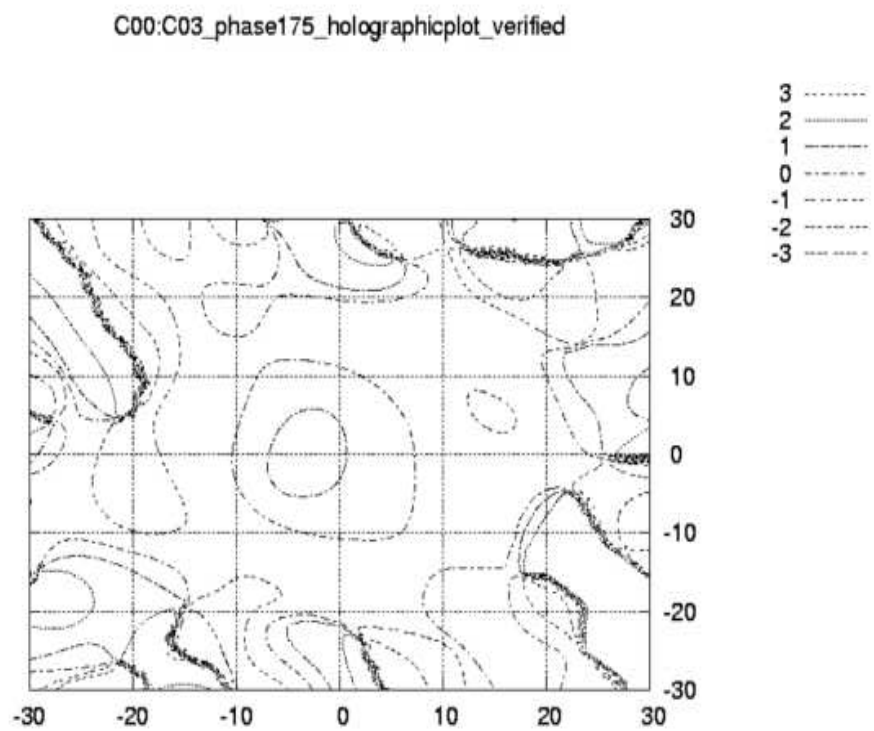


Figure 9.3: Phase At 130 and 175 for C03 with reference as C00 without feed rotation



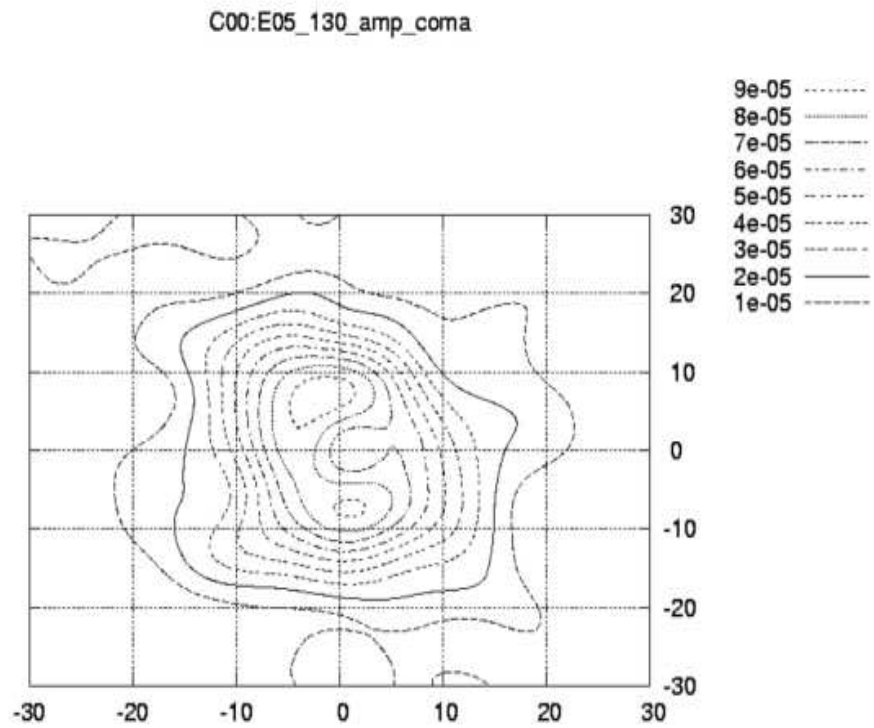
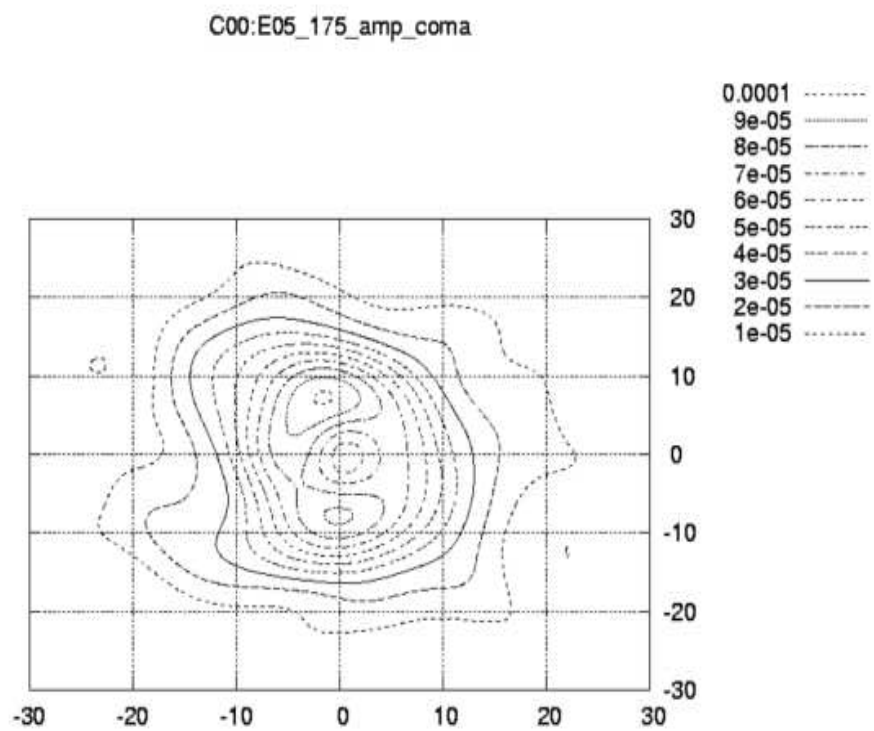


Figure 9.5: Amplitude At 130 and 175 for E05 with reference as C00 with feed rotation



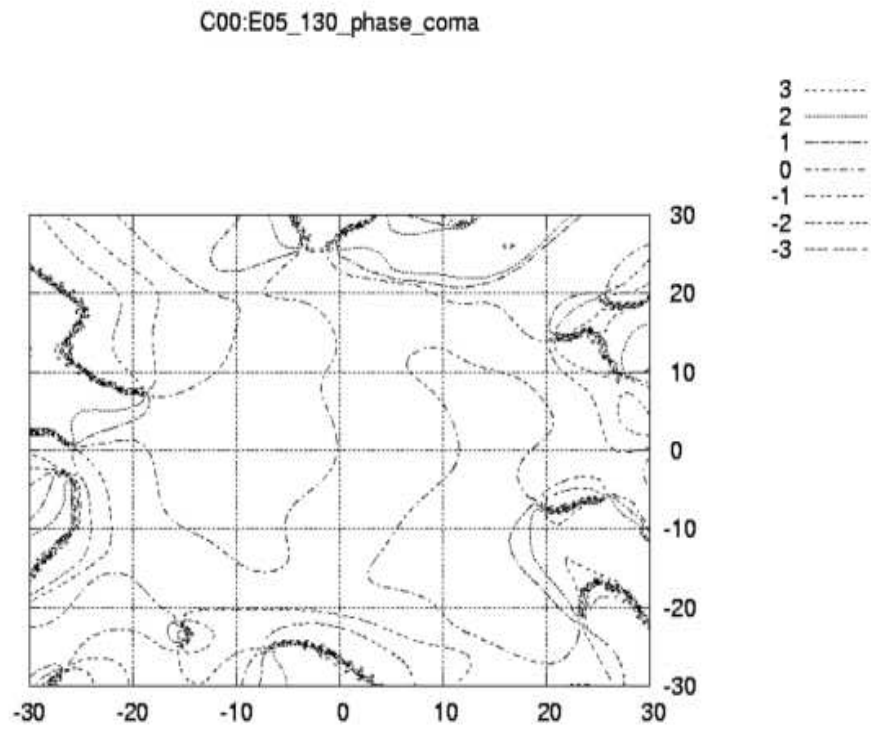
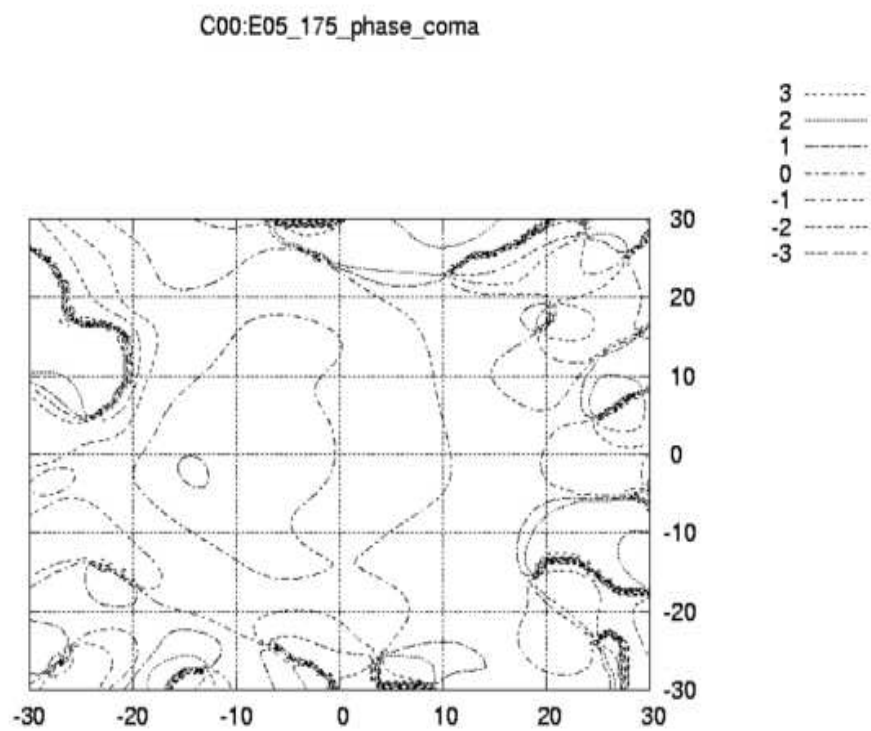


Figure 9.7: Phase At 130 and 175 for E05 with reference as C00 with feed rotation



Chapter 10

Scope of Further Development

This project was aimed to cover the basic formalism of Radio-Holographic measurements at GMRT. Even though the basic formalism has been done but still there remains a plethora of work that can be done to develop the operation. Below some of them are mentioned.

- The present resolution on the dish is about 7 meters. It can be reduced to 1 meter (which is appreciable) by taking longer scans of about 10 beamwidths.
- The algorithm that has been developed can be verified by simulating the code with a given aperture illumination with some known defects.
- The coma estimation has been started. But that too requires a deep study to figure out.
- To extract every possible defects from the aperture illumination by expansion of the circular Zernike Polynomials [6]
- The 610 MHz data has to be analysed for all the antennas.
- Holography can also be done by manually moving the feed in the vertical direction.
- The present software developed is in parts. So the most useful future work will be to merge all the program and create a single stand alone program that will take the LTA file as input and will produce holographic maps(in amplitude and phase) as its output.

Chapter 11

Codes

11.1 Fortran Code for Scanning Technique

```
* Program to evaluate the respective Azimuth and elevation Scan rate
* in different scans that suffice the Holography experiment of 14th
* December 2003, and 22nd April at GMRT.
```

```
implicit none
* all variables are in arcmin
real*8 v_alpha,v_beta,theta_n(10000),cos_el_n(10000)
real*8 theta_incr,scan_rate,start_obs,end_obs
real*8 extent,radius,time_each_scan,freq
real*8 NY_spacing,dead_time,source_transit
real*8 rate_el,rate_as,current_time,lat
real*8 hour_angle(10000),dec,sin_el,b
real*8 peak_time,beam_width,verify,res_v,stop_scan
real*8 p,D2R
integer*4 n,i,j,value

open(unit=11,file='holo_14=11.out')
open(unit=12,file='holo_14=12.out')
open(unit=13,file='holo_14=13.out')
open(unit=14,file='holo_14=34.out')

D2R = ATAN(1.0D0)/45.0D0

* Latitude of GMRT(in degree)
lat = 19.1
* Declination of the source : dec (in degrees)

write(*,*)'Enter beamwidth at frequency of obs(in deg)\'
read(*,*)b
write(11,*)'The primary beamwidth at frequency of obs(in deg)',b

write(*,*)'Enter the declination of the source(in degrees)\'
```

```
read(*,*)dec
write(11,*)'The declination of the source(in degrees) ',dec

*   current_time is in minutes
    current_time=0.0d0
    write(*,*)'Enter the starting time of observation'
    read(*,*)start_obs
    write(11,*)'The starting time of observation',start_obs

    write(*,*)'Enter the ending time of observation'
    read(*,*)end_obs
    write(11,*)'The starting time of observation',end_obs

    write(*,*)'Enter the dead time between each scans(min)'
    read(*,*)dead_time
    write(11,*)'The dead time between scans',dead_time

    write(*,*)'Observing Frequency(in MHZ) ?'
    read(*,*)freq
    write(11,*)'Observing frequency(in MHZ) is ',freq

    write(*,*)'Transit time of source(in hours) ?'
    read(*,*)source_transit
    write(11,*)'Transit time(hrs) of source ',source_transit

    write(*,*)'How many beamwidth u want to go ?'
    read(*,*)extent
    write(11,*)'NO. of beamwidth u want to go ',extent

    beam_width=b*60
*   Therefore the radius of the circular mesh is

    radius = beam_width*extent

    write(11,*)'Ans'
    write(11,*)'The radius(in arc-min) of the mesh is' , radius

    write(*,*)'No. of scans u want to take'
    read(*,*)n
    write(11,*)'No. of scans to be take',n

    write(*,*)'The resultant scan-rate(arc-min/min) u want to take'
    read(*,*)scan_rate
    write(11,*)'Resultant scan-rate(arc-min/min) u want',scan_rate
```

```

time_each_scan= 2.*radius/scan_rate
write(11,*)'Ans'
write(11,*)'Tot time(min) reqd for 1 scan',time_each_scan

*   Nyquist Sampling Spacing = lambda/ D
*   D = 45 m, diameter of the dish.

NY_spacing= ((300/freq)*(180*60/3.14))/45
write(11,*)'Ans'
write(11,*)'Nyquist Spacing(in arc-min) is ',NY_spacing
write(11,*)'Ans'
write(11,*)'Total Scans predicted by Nyquist is ',NY_spacing
*   tot= (3.14*radius)/NY-spacing
write(11,*)'Tot Time(min)for all scans ',(3.14*radius)*time_each_scan/NY_spacing
*   tot= (3.14*radius)/NY-spacing
write(11,*)'Tot Time(min)for all scans ',(3.14*radius)*time_each_scan/NY_spacing

*   theta_incr= (180*60)/n

theta_n(1)=0.

write(12,*)'scan_no', 'rate_alpha','rate_beta','res_v ','theta_n '
write(13,*)'scan_no ', 'rate_as ', 'rate_el', 'peak_time ', 'resultant_scan_rate'
write(14,*)'scan#' , 'scan_start', ' rate_as', ' rate_el', 'scan_stop', 'peak_time'
value = 1

do i=1,n+1

*   Hour Angle at transit of the source is 0

hour_angle(i)=0.-(source_transit-start_obs-((current_time+(time_each_scan/2))
1*1.002785515
* The last multiplicative factor is the corection due to the sidereal time.

sin_el=(sin(D2R*lat)*sin(D2R*dec))+cos(D2R*lat)*cos(D2R*dec)*cos(hour_angle(i))
cos_el_n(i)=dsqrt(1-(sin_el*sin_el))
write(*,*)(theta_n(i)),sin(D2R*theta_n(i)),cos(D2R*theta_n(i))
v_alpha=value*scan_rate*cos(theta_n(i)*D2R)
v_beta=value*scan_rate*sin(theta_n(i)*D2R)

res_v=dsqrt((v_alpha*v_alpha)+(v_beta*v_beta))

write(12,1)i,v_alpha,v_beta,res_v,theta_n(i)
1 format(2x,I2,7x,F8.4,5x,F8.4,6x,F8.4,6x,F8.4,2x)

```

```
    peak_time=current_time+(time_each_scan/2)

    rate_el=v_beta
    rate_as=v_alpha/cos_el_n(i)
    rate_as=v_alpha/cos_el_n(i)

    verify =dsqrt( (rate_el*rate_el)+(rate_as*rate_as))

    write(13,2)i,rate_as,rate_el,peak_time,verify
2    format(2x,I2,6x,F8.4,6x,F8.4,5x,F8.4,5x,F8.4,2x)

    stop_scan=current_time+time_each_scan
    write(14,3)i,current_time,rate_as,rate_el,stop_scan,peak_time,sin_el
3    format(2x,I2,4x,F6.2,4x,F19.13,4x,F8.4,4x,F6.2,4x,F6.2,2x,F6.2)

    value=-value
    current_time=current_time+(time_each_scan+dead_time)

*    Theta is calculated in degree

    theta_n(i+1)=(180./n)*i
    enddo
    stop
    end
```

11.2 Octave Code for Data Analysis

11.2.1 Initial Analysis

* Octave Code of the program that takes in the input as each scan(extracted from the
 * LTA file using "./xtract" program) and gives in the output all the scans after
 * Bandpass Calibration, Smoothing, Channel Collapse and well-aligned.

```
%%%%%%%%%
```

```
function initial_holography
```

```
clc;
```

```
clear;
```

```
%close;
```

```
%***** Opening Files *****
```

```
New130 = zeros(1,402);
```

```
New175 = zeros(1,402);
```

```
processed_data_130 = zeros(18,201);
```

```
processed_data_175 = zeros(18,201);
```

```
filename10 = "130.out";
```

```
filename11 = "175.out";
```

```
%***** calling each scan files for storing the skydata in an array *****
```

```
for i = 1:1:18
```

```
i
```

```
    if(i== 1)
```

```
i
```

```
    filename0 = "14dec_0_C00:C03_target_allchannel.out";
```

```
    filename1 = "14dec_0_C00:C03_ac.out";
```

```
    smoothing(filename0,filename1); % calling the function smoothing for scan0
```

```
    %****Sorting the raw-data into a single row matrix*****
```

```
    fp10 = fopen(filename10,"r");
```

```
    fp11 = fopen(filename11,"r");
```

```
    [New130 stop] = fscanf(fp10,"%f",[1,Inf]);
```

```
    [New175 stop] = fscanf(fp11,"%f",[1,Inf]);
```

```
    fclose(fp10);
```

```
    fclose(fp11);
```

```
    %*****
```

```
for k = 1:1:201
```

```
    k1 = 2*k - 1;
```

```
    k2 = 2*k ;
```

```
    processed_data_130(i,k) = New130(1,k1) + j* New130(1,k2);
```

```
    processed_data_175(i,k) = New175(1,k1) + j* New175(1,k2);
```

```
endfor
```

```
endif
```

```

if(i== 2)
i
    filename0 = "14dec_1_C00:C03_target_allchannel.out";
    filename1 = "14dec_1_C00:C03_ac.out";
    smoothing(filename0,filename1); % calling the function smoothing for scan1
    %****Sorting the raw-data into a single row matrix*****
    fp10 = fopen(filename10,"r");
    fp11 = fopen(filename11,"r");
    [New130 stop] = fscanf(fp10,"%f",[1,Inf]);
    [New175 stop] = fscanf(fp11,"%f",[1,Inf]);
    fclose(fp10);
    fclose(fp11);
    %*****
    for k = 1:1:201
        k1 = 2*k - 1;
        k2 = 2*k ;
        processed_data_130(i,k) = New130(1,k1) + j* New130(1,k2);
        processed_data_175(i,k) = New175(1,k1) + j* New175(1,k2);
    endfor
endif

if(i == 3)
i
    filename0 = "14dec_2_C00:C03_target_allchannel.out";
    filename1 = "14dec_2_C00:C03_ac.out";
    smoothing(filename0,filename1); % calling the function smoothing for scan2
    %****Sorting the raw-data into a single row matrix*****
    fp10 = fopen(filename10,"r");
    fp11 = fopen(filename11,"r");
    [New130 stop] = fscanf(fp10,"%f",[1,Inf]);
    [New175 stop] = fscanf(fp11,"%f",[1,Inf]);
    fclose(fp10);
    fclose(fp11);
    %*****
    for k = 1:1:201
        k1 = 2*k - 1;
        k2 = 2*k ;
        processed_data_130(i,k) = New130(1,k1) + j* New130(1,k2);
        processed_data_175(i,k) = New175(1,k1) + j* New175(1,k2);
    endfor
endif

if(i== 4)
i
    filename0 = "14dec_3_C00:C03_target_allchannel.out";
    filename1 = "14dec_3_C00:C03_ac.out";
    smoothing(filename0,filename1); % calling the function smoothing for scan3

```

```

%***Sorting the raw-data into a single row matrix*****
fp10 = fopen(filename10,"r");
fp11 = fopen(filename11,"r");
[New130 stop] = fscanf(fp10,"%f",[1,Inf]);
[New175 stop] = fscanf(fp11,"%f",[1,Inf]);
fclose(fp10);
fclose(fp11);
%*****
for k = 1:1:201
    k1 = 2*k - 1;
    k2 = 2*k ;
    processed_data_130(i,k) = New130(1,k1) + j* New130(1,k2);
    processed_data_175(i,k) = New175(1,k1) + j* New175(1,k2);
endfor
endif

if(i==5)
i
    filename0 = "14dec_4_C00:C03_target_allchannel.out";
    filename1 = "14dec_4_C00:C03_ac.out";
    smoothing(filename0,filename1); % calling the function smoothing for scan4
%***Sorting the raw-data into a single row matrix*****
fp10 = fopen(filename10,"r");
fp11 = fopen(filename11,"r");
[New130 stop] = fscanf(fp10,"%f",[1,Inf]);
[New175 stop] = fscanf(fp11,"%f",[1,Inf]);
fclose(fp10);
fclose(fp11);
%*****
for k = 1:1:201
    k1 = 2*k - 1;
    k2 = 2*k ;
    processed_data_130(i,k) = New130(1,k1) + j* New130(1,k2);
    processed_data_175(i,k) = New175(1,k1) + j* New175(1,k2);
endfor
endif

if(i== 6)
i
    filename0 = "14dec_5_C00:C03_target_allchannel.out";
    filename1 = "14dec_5_C00:C03_ac.out";
    smoothing(filename0,filename1); % calling the function smoothing for scan5
%***Sorting the raw-data into a single row matrix*****
fp10 = fopen(filename10,"r");
fp11 = fopen(filename11,"r");
[New130 stop] = fscanf(fp10,"%f",[1,Inf]);
[New175 stop] = fscanf(fp11,"%f",[1,Inf]);

```



```

fclose(fp10);
fclose(fp11);
%*****
for k = 1:1:201
    k1 = 2*k - 1;
    k2 = 2*k ;
    processed_data_130(i,k) = New130(1,k1) + j* New130(1,k2);
    processed_data_175(i,k) = New175(1,k1) + j* New175(1,k2);
endfor
endif

if(i==7)
i
    filename0 = "14dec_6_C00:C03_target_allchannel.out";
    filename1 = "14dec_6_C00:C03_ac.out";
    smoothing(filename0,filename1); % calling the function smoothing for scan6
    %****Sorting the raw-data into a single row matrix*****
    fp10 = fopen(filename10,"r");
    fp11 = fopen(filename11,"r");
    [New130 stop] = fscanf(fp10,"%f",[1,Inf]);
    [New175 stop] = fscanf(fp11,"%f",[1,Inf]);
    fclose(fp10);
    fclose(fp11);
    %*****
    for k = 1:1:201
        k1 = 2*k - 1;
        k2 = 2*k ;
        processed_data_130(i,k) = New130(1,k1) + j* New130(1,k2);
        processed_data_175(i,k) = New175(1,k1) + j* New175(1,k2);
    endfor
endif

if(i== 8)
i
    filename0 = "14dec_7_C00:C03_target_allchannel.out";
    filename1 = "14dec_7_C00:C03_ac.out";
    smoothing(filename0,filename1); % calling the function smoothing for scan7
    %****Sorting the raw-data into a single row matrix*****
    fp10 = fopen(filename10,"r");
    fp11 = fopen(filename11,"r");
    [New130 stop] = fscanf(fp10,"%f",[1,Inf]);
    [New175 stop] = fscanf(fp11,"%f",[1,Inf]);
    fclose(fp10);
    fclose(fp11);
    %*****
    for k = 1:1:201
        k1 = 2*k - 1;

```

```

        k2 = 2*k ;
        processed_data_130(i,k) = New130(1,k1) + j* New130(1,k2);
        processed_data_175(i,k) = New175(1,k1) + j* New175(1,k2);
    endfor
endif

if(i== 9)
i
    filename0 = "14dec_8_C00:C03_target_allchannel.out";
    filename1 = "14dec_8_C00:C03_ac.out";
    smoothing(filename0,filename1); % calling the function smoothing for scan8
    %****Sorting the raw-data into a single row matrix*****
    fp10 = fopen(filename10,"r");
    fp11 = fopen(filename11,"r");
    [New130 stop] = fscanf(fp10,"%f",[1,Inf]);
    [New175 stop] = fscanf(fp11,"%f",[1,Inf]);
    fclose(fp10);
    fclose(fp11);
    %*****
    for k = 1:1:201
        k1 = 2*k - 1;
        k2 = 2*k ;
        processed_data_130(i,k) = New130(1,k1) + j* New130(1,k2);
        processed_data_175(i,k) = New175(1,k1) + j* New175(1,k2);
    endfor
endif

if(i== 10)
i
    filename0 = "14dec_9_C00:C03_target_allchannel.out";
    filename1 = "14dec_9_C00:C03_ac.out";
    smoothing(filename0,filename1); % calling the function smoothing for scan9
    %****Sorting the raw-data into a single row matrix*****
    fp10 = fopen(filename10,"r");
    fp11 = fopen(filename11,"r");
    [New130 stop] = fscanf(fp10,"%f",[1,Inf]);
    [New175 stop] = fscanf(fp11,"%f",[1,Inf]);
    fclose(fp10);
    fclose(fp11);
    %*****
    for k = 1:1:201
        k1 = 2*k - 1;
        k2 = 2*k ;
        processed_data_130(i,k) = New130(1,k1) + j* New130(1,k2);
        processed_data_175(i,k) = New175(1,k1) + j* New175(1,k2);
    endfor
endif

```

```

if(i== 11)
i
    filename0 = "14dec_10_C00:C03_target_allchannel.out";
    filename1 = "14dec_10_C00:C03_ac.out";
    smoothing(filename0,filename1); % calling the function smoothing for scan10
    %***Sorting the raw-data into a single row matrix*****
    fp10 = fopen(filename10,"r");
    fp11 = fopen(filename11,"r");
    [New130 stop] = fscanf(fp10,"%f",[1,Inf]);
    [New175 stop] = fscanf(fp11,"%f",[1,Inf]);
    fclose(fp10);
    fclose(fp11);
    %*****
    for k = 1:1:201
        k1 = 2*k - 1;
        k2 = 2*k ;
        processed_data_130(i,k) = New130(1,k1) + j* New130(1,k2);
        processed_data_175(i,k) = New175(1,k1) + j* New175(1,k2);
    endfor
endif

if(i== 12)
i
    filename0 = "14dec_11_C00:C03_target_allchannel.out";
    filename1 = "14dec_11_C00:C03_ac.out";
    smoothing(filename0,filename1); % calling the function smoothing for scan11
    %***Sorting the raw-data into a single row matrix*****
    fp10 = fopen(filename10,"r");
    fp11 = fopen(filename11,"r");
    [New130 stop] = fscanf(fp10,"%f",[1,Inf]);
    [New175 stop] = fscanf(fp11,"%f",[1,Inf]);
    fclose(fp10);
    fclose(fp11);
    %*****
    for k = 1:1:201
        k1 = 2*k - 1;
        k2 = 2*k ;
        processed_data_130(i,k) = New130(1,k1) + j* New130(1,k2);
        processed_data_175(i,k) = New175(1,k1) + j* New175(1,k2);
    endfor
endif

if(i== 13)
i
    filename0 = "14dec_12_C00:C03_target_allchannel.out";
    filename1 = "14dec_12_C00:C03_ac.out";
    smoothing(filename0,filename1); % calling the function smoothing for scan12

```

```

%***Sorting the raw-data into a single row matrix*****
fp10 = fopen(filename10,"r");
fp11 = fopen(filename11,"r");
[New130 stop] = fscanf(fp10,"%f",[1,Inf]);
[New175 stop] = fscanf(fp11,"%f",[1,Inf]);
fclose(fp10);
fclose(fp11);
%*****
for k = 1:1:201
    k1 = 2*k - 1;
    k2 = 2*k ;
    processed_data_130(i,k) = New130(1,k1) + j* New130(1,k2);
    processed_data_175(i,k) = New175(1,k1) + j* New175(1,k2);
endfor
endif

if(i==14)
i
    filename0 = "14dec_13_C00:C03_target_allchannel.out";
    filename1 = "14dec_13_C00:C03_ac.out";
    smoothing(filename0,filename1); % calling the function smoothing for scan13
%***Sorting the raw-data into a single row matrix*****
fp10 = fopen(filename10,"r");
fp11 = fopen(filename11,"r");
[New130 stop] = fscanf(fp10,"%f",[1,Inf]);
[New175 stop] = fscanf(fp11,"%f",[1,Inf]);
fclose(fp10);
fclose(fp11);
%*****
for k = 1:1:201
    k1 = 2*k - 1;
    k2 = 2*k ;
    processed_data_130(i,k) = New130(1,k1) + j* New130(1,k2);
    processed_data_175(i,k) = New175(1,k1) + j* New175(1,k2);
endfor
endif
if(i==15)
i
    filename0 = "14dec_14_C00:C03_target_allchannel.out";
    filename1 = "14dec_14_C00:C03_ac.out";
    smoothing(filename0,filename1); % calling the function smoothing for scan14
%***Sorting the raw-data into a single row matrix*****
fp10 = fopen(filename10,"r");
fp11 = fopen(filename11,"r");
[New130 stop] = fscanf(fp10,"%f",[1,Inf]);
[New175 stop] = fscanf(fp11,"%f",[1,Inf]);
fclose(fp10);

```

```

fclose(fp11);
%*****
for k = 1:1:201
    k1 = 2*k - 1;
    k2 = 2*k ;
    processed_data_130(i,k) = New130(1,k1) + j* New130(1,k2);
    processed_data_175(i,k) = New175(1,k1) + j* New175(1,k2);
endfor
endif
if(i==16)
i
    filename0 = "14dec_15_C00:C03_target_allchannel.out";
    filename1 = "14dec_15_C00:C03_ac.out";
    smoothing(filename0,filename1); % calling the function smoothing for scan15
%****Sorting the raw-data into a single row matrix*****
    fp10 = fopen(filename10,"r");
    fp11 = fopen(filename11,"r");
    [New130 stop] = fscanf(fp10,"%f",[1,Inf]);
    [New175 stop] = fscanf(fp11,"%f",[1,Inf]);
    fclose(fp10);
    fclose(fp11);
%*****
    for k = 1:1:201
        k1 = 2*k - 1;
        k2 = 2*k ;
        processed_data_130(i,k) = New130(1,k1) + j* New130(1,k2);
        processed_data_175(i,k) = New175(1,k1) + j* New175(1,k2);
    endfor
endif

if(i==17)
i
    filename0 = "14dec_16_C00:C03_target_allchannel.out";
    filename1 = "14dec_16_C00:C03_ac.out";
    smoothing(filename0,filename1); % calling the function smoothing for scan16
%****Sorting the raw-data into a single row matrix*****
    fp10 = fopen(filename10,"r");
    fp11 = fopen(filename11,"r");
    [New130 stop] = fscanf(fp10,"%f",[1,Inf]);
    [New175 stop] = fscanf(fp11,"%f",[1,Inf]);
    fclose(fp10);
    fclose(fp11);
%*****
    for k = 1:1:201
        k1 = 2*k - 1;
        k2 = 2*k ;
        processed_data_130(i,k) = New130(1,k1) + j* New130(1,k2);

```

```

        processed_data_175(i,k) = New175(1,k1) + j* New175(1,k2);
    endfor
endif

if(i==18)
i
    filename0 = "14dec_17_C00:C03_target_allchannel.out";
    filename1 = "14dec_17_C00:C03_ac.out";
    smoothing(filename0,filename1); % calling the function smoothing for scan17
    %****Sorting the raw-data into a single row matrix*****
    fp10 = fopen(filename10,"r");
    fp11 = fopen(filename11,"r");
    [New130 stop] = fscanf(fp10,"%f",[1,Inf]);
    [New175 stop] = fscanf(fp11,"%f",[1,Inf]);
    fclose(fp10);
    fclose(fp11);
    %*****
    for k = 1:1:201
        k1 = 2*k - 1;
        k2 = 2*k ;
        processed_data_130(i,k) = New130(1,k1) + j* New130(1,k2);
        processed_data_175(i,k) = New175(1,k1) + j* New175(1,k2);
    endfor
endif

endfor
%*****
*****Printing to File *****
filename20 = "intial_data_130.hol";
filename21 = "initial_data_175.hol";
fp20 = fopen(filename20,"w");
fp21 = fopen(filename21,"w");
for m =1:1:18
    for n =1:1:201
        fprintf(fp20,"%f %f \n",real(processed_data_130(m,n)),imag(processed_data_130(m,n)
        fprintf(fp21,"%f %f \n",real(processed_data_175(m,n)),imag(processed_data_175(m,n)
    endfor
endfor
fclose(fp20);
fclose(fp21);

%*****
endfunction
function smoothing(filename0,filename1)
****Sorting the raw-data into a single row matrix*****
fp0 = fopen(filename0,"r");
filename0

```

```

filename1
uptostring("#","0",fp0); %reaching the last char string "#0"
uptochar("\n", fp0 );    %reaching the end of the line

[rawdata stop] = fscanf(fp0,"%f",[1,Inf]);

fclose(fp0);
%*****
[M N] = size(rawdata) ;

data_real_130_0 = zeros(1,128);
data_im_130_0 = zeros(1,128);
data_real_175_0 = zeros(1,128);
data_im_175_0 = zeros(1,128);
i = 1;
k = 1;
for m = 2:2:N
    if(m < 258)
data_real_130_0(1,i) = rawdata(1,m);
data_im_130_0(1,i) = rawdata(1,m+1);
        i = i + 1;
    endif
    if(m >= 258 )
        data_real_175_0(1,k) = rawdata(1,m);
data_im_175_0(1,k) = rawdata(1,m+1);
        k = k+1;
    endif
endfor
rawdata = []; %killing the rawdata matrix
%#####
Ant130_0 = data_real_130_0+ j*data_im_130_0;
Ant175_0 = data_real_175_0+ j*data_im_175_0;
Xaxis = 1:1:128;
##### End of File 1 #####

***** Calculations *****
for i =1:1:100

calib_130(i) = arg(Ant130_0(i+10));
calib_175(i) = arg(Ant175_0(i+10));
endfor
rescalib_130 = detrend (calib_130,1);
rescalib_175 = detrend (calib_175,1);
for i = 1:1:100
smooth_130(i) = calib_130(i) - rescalib_130 (i);
smooth_175(i) = calib_175(i) - rescalib_175 (i);
endfor

```

```

%*****
Xaxis1 = 1:1:100;

***** Beginning the Channel calibration for each scans *****

****Sorting the raw-data into a single row matrix*****
fp1 = fopen(filename1,"r");

uptostring("#","0",fp1); %reaching the last char string "#0"
uptochar("\n", fp1 ); %reaching the end of the line

[rawdata stop] = fscanf(fp1,"%f",[1,Inf]);

fclose(fp1);
*****
Col=401;
[M N] = size(rawdata) ;
Rows =N/Col;

i = 1;
data = zeros(Rows,Col);
for m = 1:1:Rows
for n = 1:1:Col
data(m,n) = rawdata(1,i);
i = i + 1;
endfor
endfor

rawdata =[]; %killing the rawdata matrix

[M1 N1] = size( data ) ;
avg_data = zeros(M1,5);
cal_data = zeros(M1,5);
phase_diff = zeros(M1,5);

    for m = 1:1:M1

ir=1;
k=1;

        for n=2:2:N1
            avg_data(m,1)=data(m,1);

                if(n <= 201)

cal_data(m,1) = data(m,n) + j*data(m,n+1);

```



```

        phase_diff(m,1) = arg(cal_data(m,1)) - smooth_130(ir);

nval_real = abs(cal_data(m,1))*cos(phase_diff(m,1));
nval_imag = abs(cal_data(m,1))*sin(phase_diff(m,1));

        avg_data(m,2) = avg_data(m,2) + nval_real;
        avg_data(m,3) = avg_data(m,3) + nval_imag;
ir= ir+1;
        endif

if(n >= 202)

        cal_data(m,2) = data(m,n) + j*data(m,n+1);
        phase_diff(m,2)= arg(cal_data(m,2)) - smooth_175(k);

        nval_real = abs(cal_data(m,1))*cos(phase_diff(m,1));
nval_imag = abs(cal_data(m,1))*sin(phase_diff(m,1));

        avg_data(m,4) = avg_data(m,4) + nval_real;
        avg_data(m,5) = avg_data(m,5) + nval_imag;

        k=k+1;
        endif

endfor
        avg_data(m,2)= avg_data(m,2)/100;
        avg_data(m,3)=avg_data(m,3)/100;
        avg_data(m,4)=avg_data(m,4)/100;
        avg_data(m,5)=avg_data(m,5)/100;
endfor

****Sorting the data into time, ant-USB & ant-LSB (re + j im)****
TimeStamp = avg_data(:,1)';
Ant130 = avg_data(:,2)' + j*avg_data(:,3)';
[orig_row orig_col] = size(Ant130);
Ant130 = [zeros(1,250),Ant130,zeros(1,250)];

Ant175 = avg_data(:,4)' + j*avg_data(:,5)';
Ant175 = [zeros(1,250),Ant175,zeros(1,250)];

***** Analysis *****
FFT130 = fft(Ant130);

```

```

Mag130 = abs(FFT130);

FFT175 = fft(Ant175);
Mag175 = abs(FFT175);

[M10 N10] = size(Mag130);
Xaxis2 = 1:1:N10;
 %[M11 N11] = size(Xaxis2)

BW = .1;
nn = round(N10*BW);
ONES = ones(1, nn);
kk = N10 - 2*nn;
PadMat = [ ONES, zeros(1,kk), ONES ];

PFFT130 = FFT130.*PadMat;
PFFT175 = FFT175.*PadMat;

IFFT130 = ifft(PFFT130);
IFFT175 = ifft(PFFT175);

[M8 N8] = size(IFFT130) ;
[Max130 ind130] = max(IFFT130);
[Max175 ind175] = max(IFFT175);
*****
Resizing of the scan arrays and normalising

New130 = zeros(1,201);
New175 = zeros(1,201);
Xaxis10 = 1:1:201;

k1= 251;
for i = 1:1:201

    if(i <= (101 - ( ind130 - 250)))
        New130(1,i) = 0;
    endif
    if(i > (101 - ( ind130 - 250)))
        New130(1,i) = IFFT130(k1);
        k1 = k1+1;
    endif

endfor
k2= 251;
for i = 1:1:201

    if(i <= (101 - ( ind175 - 250)))

```

```
        New175(1,i) = 0;
    endif
    if(i > (101 - ( ind175 - 250)))
        New175(1,i) = IFFT175(k2);
        k2 = k2+1;
    endif
endfor
%New130
%New175
phase130 = arg(New130(1,101));
phase175 = arg(New175(1,101));
amp130 = abs(New130(1,101));
amp175 = abs(New175(1,101));
ind = 102 - ( ind130 - 250) + orig_col;
for i = (102 - ( ind130 - 250)):1:201
    if(i <= (102 - ( ind130 - 250) +orig_col))
        phase_cur130= arg(New130(1,i)) - phase130 ;
        abs_cur130 = abs(New130(1,i))/amp130 ;

        re_cur130 = abs_cur130 * cos(phase_cur130);
        im_cur130 = abs_cur130 * sin(phase_cur130);

        cplx_cur130 = re_cur130 + j*im_cur130;

        New130(1,i) = cplx_cur130;
    endif
    if(i > (102 - ( ind130 - 250) +orig_col))
        New130(1,i) = 0 + 0*j;
    endif
endfor

for i = (102 - ( ind175 - 250)):1:201
    if(i <= (102 - ( ind175 - 250) +orig_col))
        phase_cur175 = arg(New175(1,i)) - phase175;
        abs_cur175 = abs(New175(1,i))/amp175 ;

        re_cur175 = abs_cur175 * cos(phase_cur175);
        im_cur175 = abs_cur175 * sin(phase_cur175);

        cplx_cur175 = re_cur175 + j*im_cur175;

        New175(1,i) = cplx_cur175;
    endif
    if(i > (102 - ( ind175 - 250) +orig_col))
        New175(1,i) = 0 + 0*j;
    endif
endfor
```

```

endfor
%New130

*****Printing to File *****
filename10="130.out";
filename11="175.out";

fp10 = fopen(filename10,"w");
fp11 = fopen(filename11,"w");
for m =1:1:201
    fprintf(fp10,"%f %f \n",real(New130(1,m)),imag(New130(1,m)) );
    fprintf(fp11,"%f %f \n",real(New175(1,m)),imag(New175(1,m)) );
endfor
fclose(fp10);
fclose(fp11);

endfunction
#####
function uptochar( lastchar, fp1 )
    tmpchar = '';
    while ( tmpchar != lastchar )
        tmpchar = fgets(fp1,1);
    endwhile
endfunction
#####
function uptostring( c1,c2, fp2 )

    tt = 0;
    while(tt == 0 )
        uptochar( c1, fp2 );
        tmpchar = fgets( fp2, 1);
        if (tmpchar == c2 )
            tt = 1;
        endif
    endwhile

endfunction
#####
\subsection[\large{Final Analysis}]{\large{\textbf{Final Analysis}}}
* Octave code that takes the output of initinal_holography
* and then computes the aperture distribution by using the
* direct Fourier Transform

function final_holography

filename20 = "intial_data_130.hol";

```

```

filename21 = "initial_data_175.hol";
processed_data_130=zeros(18,201);
processed_data_175=zeros(18,201);

    %****Sorting the raw-data into a single row matrix*****
    fp20 = fopen(filename20,"r");
    fp21 = fopen(filename21,"r");
    [New130 stop] = fscanf(fp20,"%f",[1,Inf]);
    [New175 stop] = fscanf(fp21,"%f",[1,Inf]);
    fclose(fp20);
    fclose(fp21);
    %*****
n=1
for k=1:1:18
    for i=1:1:201
        processed_data_130(k,i) = New130(1,n)+j*New130(1,n+1);
        processed_data_175(k,i) = New175(1,n)+j*New175(1,n+1);
        n=n+2;
    endfor
endfor

% creating the mesh of the dish with 1 m accuracy.
xgrid_dish = zeros(1,61);
ygrid_dish = zeros(1,61);
delta =1;% distance in meters
delta
xgrid_dish(1,1) = -(30*delta);
ygrid_dish(1,1) = -(30*delta);

for i = 2:1:61
    k = i - 1;
    xgrid_dish(1,i) = xgrid_dish(1,k) + delta ;
    ygrid_dish(1,i) = ygrid_dish(1,k) + delta ;
endfor
120000
xgrid_dish
ygrid_dish
zgrid_dish_130 = zeros(61,61); % creating the grid consisting the field-value
zgrid_dish_175 = zeros(61,61);
%*****-----

%***** Direct Fourier transform *****
factor = 0.;
Lambda = 0.23438; % wavelength of observation in meters
FT_Tot_130 = 0.;
FT_Scan_130 = 0.;
FT_Tot_175 = 0.;

```

```

FT_Scan_175 = 0.;
rad = pi/(180*60);
rad1 = pi/180;
delta_theta = 252./100; % tot. arcmin coverage / total points in a scan
Nscan = 18; % total no. of scans taken
delta_alpha = 180./Nscan;
for px = 1:1:61
%xgrid_dish(1,px)
  for py = 1:1:61
FT_Tot_130 = 0.;
FT_Tot_175 = 0.;
% ygrid_dish(1,py)
  sign = -1;
  alpha = 0.;
  for k = 1:1:Nscan
FT_Scan_130 = 0.;
FT_Scan_175 = 0.;

    k;
    theta = sign.*delta_theta.*50;
    wx =1;
    for i=1:2:201
    i;
    theta;
    theta_x = theta*cos(alpha*rad1);
    theta_y = theta*sin(alpha*rad1);

    weightage=abs(delta_alpha*(theta*delta_theta)* (rad1*rad*rad));
    if(i==101)
      weightage = abs((pi./4)*delta_theta*delta_theta*(rad*rad)/Nscan);
    endif
    w(1,wx) = weightage;
    factor = exp(j*(2*pi)*((xgrid_dish(1,px).*theta_x*rad)+(ygrid_dish(1,py).*theta_y*rad)));

    FT_Scan_130 = FT_Scan_130+(processed_data_130(k,i).*weightage*factor);
    FT_Scan_175 = FT_Scan_175+(processed_data_175(k,i).*weightage*factor);

    theta = theta - sign*delta_theta;
    wx = wx +1;
  endfor

  alpha = alpha + delta_alpha;
  % difference in alpha for each scan than the previous
  sign = - sign; % changing of sign due to the scanning technique

```

```

    FT_Tot_130 = FT_Tot_130 + FT_Scan_130;
    FT_Tot_175 = FT_Tot_175 + FT_Scan_175;
endfor

    zgrid_dish_130(px,py) = FT_Tot_130;
    zgrid_dish_175(px,py) = FT_Tot_175;

endfor
endfor
zgrid_dish_130;
w
Xaxis=1:1:16;

figure(1);

contour(xgrid_dish,ygrid_dish,abs(zgrid_dish_130));
figure(2);
mesh(xgrid_dish,ygrid_dish,abs(zgrid_dish_130));

IFF130=ifft2(zgrid_dish_130);
IF130=fftshift(IFF130);
figure(10);
mesh(xgrid_dish,ygrid_dish,abs(IF130));

figure(3);
contour(xgrid_dish,ygrid_dish,abs(zgrid_dish_175));
figure(4);
mesh(xgrid_dish,ygrid_dish,abs(zgrid_dish_175));
figure(5);
contour(xgrid_dish,ygrid_dish,arg(zgrid_dish_130));
figure(6);
mesh(xgrid_dish,ygrid_dish,arg(zgrid_dish_130));
figure(7);
contour(xgrid_dish,ygrid_dish,arg(zgrid_dish_175));
figure(8);
mesh(xgrid_dish,ygrid_dish,arg(zgrid_dish_175));
figure(5)
%plot(Xaxis,abs(zgrid_dish_130(1,:)), 'r',abs(zgrid_dish_175(1,:)), 'b');
%figure(6)
%plot(Xaxis,arg(zgrid_dish_130(1,:)), 'r',arg(zgrid_dish_175(1,:)), 'b');
figure(11);
plot(w);
%endfunction
%*****Printing to File *****

```

```
filename20 = "final_data_130+175_C00:C03.hol";
fp20 = fopen(filename20,"w");
for m =1:1:61
  for n =1:1:61
fprintf(fp20,"%f %f %f %f \n",real(zgrid_dish_130(m,n)), imag(zgrid_dish_130(m,n))

  endfor
endfor
fclose(fp20);

endfunction
%*****
```


Bibliography

- [1] A.Richard Thompson, James M.Moran and George W.Swenson Jr: *Interferometry and Synthesis in Radio Astronomy*, John Wiley Sons. Inc, 2nd Edition(2001).
- [2] K.Rohlfs and T.L.Wilson: *Tools of Radio Astronomy*, Springer-Verlag, 2nd Edition(1996).
- [3] Ronald N.Bracewell: *The Fourier Transform and its Applications* MacGraw-Hill Book Company, 2nd Edition(1986).
- [4] Philip R.Bewington:*Data Reduction and Error Analysis for the Physical Sciences*, MacGraw-Hill Book Company(1969).
- [5] C.A. Balanis: *Antenna Theory - Analysis and Design*, John Wiley Sons (Asia) Pte LTD.
- [6] Max Born and Emil Wolf: *Principles of Optics*, 6th Edition, Cambridge University Press(1980).
- [7] John D.Kraus: *Radio Astronomy*, 2nd Edition, Cygnus-Quasar Books(1986).
- [8] P.F.Scott and M.Ryle: *A rapid method for measuring the figure of a radio telescope reflector*, Monthly Notices of Royal Astronomical Society(1977) *Vol-178*, Pages: 539-545.
- [9] J.C.Bennett, A.P.Anderson, Peter A.McInnes and A.J.T.Whitaker: *Microwave Holographic Metrology of Large Reflector Antennas*, IEEE Trans. Ant. Prop.(1976) *Vol-AP-24, No-3* Pages- 295-303.
- [10] D.Morris: *Phase Retrieval in the Radio Holography of Reflector Antennas and Radio Telescopes*, IEEE Trans. Ant. Prop.(1985), *Vol- AP-33* pages 749-755.
- [11] William L.Peters *Surface Measurements of Large Antennas At High Accuracy*, hawk.iszf.irk.ru/URSI2002/GAabstracts/papers/p0964.pdf
- [12] E.Serabyn, T.G.Philips and C.R.Mason: *Surface Figure Measurements of Radio Telescopes with a Shearing Interferometer* Applied Optics(1991), vol. 30, pages 1227-1241.